1994

Photon energy response calculations for filtered $CaSO_4$:Dy dosimeters using the EGS4 Monte Carlo code

Christopher J. Miles
San Jose State University

PHOTON ENERGY RESPONSE CALCULATIONS FOR FILTERED $CaSO_4$:Dy DOSIMETERS USING THE EGS4 MONTE CARLO CODE

A Thesis

Presented to

The Faculty of the Nuclear Science Program

San Jose State University

In Partial Fulfillment

of the Requirements for the Degree

Master of Science

by

Christopher J. Miles

December 1994

APPROVED FOR THE DEPARTMENT OF NUCLEAR SCIENCE

Dr. Peter A. J. Englert

Dr. James C. Liu

Dr. Allen B. Tucker

APPROVED FOR THE UNIVERSITY

ABSTRACT

PHOTON ENERGY RESPONSE CALCULATIONS FOR FILTERED $CaSO_4$:Dy DOSIMETERS USING THE EGS4 MONTE CARLO CODE

by Christopher J. Miles

Since the response of $CaSO_4$:Dy is not air-equivalent, filtration or other energy correction methods are necessary if dosimeters are to be exposed to low energy photons. The response of an environmental dosimeter utilizing $CaSO_4$:Dy with a brass or cadmium energy compensation filter has been studied. Experimental data were obtained by exposing $CaSO_4$:Dy powder with metal filters to photons of a few different energies. The measured dosimeter responses were compared with those calculated based on simple linear attenuation and those calculated based on EGS4 Monte Carlo simulations. The EGS4-calculated results were in closer agreement with the experimental data than the calculations based on attenuation. Discrepancies in the calculations as compared to experimental measurements are believed to be due to the energy dependent thermoluminescent efficiency of the phosphor.

ACKNOWLEDGMENTS

First and foremost, I would like to thank J. C. Liu of SLAC for his efforts in helping to prepare and troubleshoot the EGS4 user code and for the numerous hours that he spent working with me on every aspect of this study. I am also grateful to W. R. Nelson of SLAC, who inspired this work by introducing me to Monte Carlo methods and helped to get me started with the EGS4 code. Thanks are also extended to C. D. Hooker and K. K. Large of PNL for making the x-ray exposures, and to Radiation Detection Company for supporting the experimental portion of this work. I am also grateful to N. McElroy and P. A. J. Englert of SJSU for their encouragement and support, and E. T. Ochi of LLNL for his assisistance in preparing this document. Lastly, I would like to thank my wife for putting up with me throughout this process.

TABLE OF CONTENTS

APPENDICES

LIST OF TABLES

LIST OF FIGURES

1. INTRODUCTION

1.1 Background

Due primarily to man's use of nuclear technologies, the need for accurate and reliable measurements of environmental radiation and radioactivity has increased steadily over the past few decades. Measurements of ionizing radiation in the environment are required in order to assess personnel exposure to natural and manmade radiation sources and to determine compliance with government regulations. Dosimeters utilizing the phenomenon of thermoluminescence have dominated the field of environmental radiation dosimetry for many years.

1.2 Thermoluminescence

The term thermoluminescence (TL) refers to thermally stimulated light emission following excitation. Excitation may be due to optical photons, friction from rubbing or grinding, chemical reactions, electric fields, or ionizing radiation. In this paper, the term thermoluminescence refers to the case when excitation is due to ionizing radiation.

A simple model is commonly used to explain the TL process. In a perfect crystal, the outer atomic electron energy levels are divided into two "allowed" energy bands separated by "forbidden" energy regions. The highest filled band is called the valence band. It is separated by several electron volts from the lowest unfilled band called the conduction band. Ionizing radiation will excite electrons from the valence band to the conduction band, leaving vacancies in the valence band called holes. Electrons and holes are free to

move independently through their respective bands. The presence of impurities in the crystal gives rise to discrete local energy levels in the forbidden band that can trap electrons or holes. When TL material is exposed to ionizing radiation, some of the liberated electrons or holes are trapped at crystal lattice imperfections. Most TL crystals contain about 10^{16} traps per cm^3. This number of traps can be produced by only a few parts per million of impurities which cause lattice imperfections (Horowitz 1984).

Electrons or holes may remain trapped at crystal imperfections for long periods at room temperature. If the temperature is raised by heating the crystal, the electrons or holes are thermally released from the traps, resulting in the emission of light. This is referred to as TL. In TL dosimetry (TLD), the total quantity of light emitted as the material is heated is proportional to the absorbed radiation dose in the material. The heating process empties the traps so that the crystal can in theory be reused indefinitely. In practice, special annealing procedures are generally required to restore crystals to their original state and TL efficiency is a function of irradiation history and thermal history.

A plot of the emitted light intensity vs. temperature is referred to as the TL glow curve. Different TL materials have unique glow curves with light emission peaks appearing at various temperatures corresponding to trap depths. A glow curve may consist of a single peak or many peaks.

The readout instrumentation generally used in TL measurements consists of a heating mechanism coupled to a photomultiplier (PM) tube. The TL material is placed on a planchet which is heated resistively or using hot gas. In order to reduce non radiation-induced TL that can occur due to

chemiluminescence caused by oxygen in air, dosimeters are normally heated in an atmosphere of inert nitrogen gas during readout. The planchet temperature is controlled by a thermocouple in close thermal contact. The light emitted from the TL material passes through an infrared filter and a collecting lens focuses the light on the photocathode of the photomultiplier. The signal from the PM tube is then amplified and sent to a scaler that will display the digital response in units of nanocoulombs which is proportional to the TL output or radiation absorbed dose. Most modern instruments are connected with a computer where information such as glow curves may be displayed and stored.

1.3 ANSI N545-1975

In response to a need for accurate, sensitive, and reliable dosimeters for monitoring environmental radiation, an American National Standard was prepared, entitled "Performance, Testing, and Procedural Specifications for Thermoluminescence Dosimetry (Environmental Applications)" (ANSI 1975).

The standard specifies performance criteria for TLD systems used for the measurement of environmental exposure levels of X and gamma radiation. It specifies minimum acceptable performance criteria for TLD systems used for environmental measurements, outlines methods to test TLD systems and provides procedures for calibration, field application and reporting.

One of the dosimeter performance criteria specified in ANSI N545-1975 relates to energy dependence: "The response of the TLD to photons shall be

determined for several energies between 30 keV and 3 MeV. The response shall not differ from that obtained with the calibration source by more than 20% for photons with energies greater than 80 keV and shall not be enhanced by more than a factor of two for photons with energies less than 80 keV."

1.4 Objective

The primary focus of this effort has been to investigate the use of a Monte Carlo code to design dosimeters that will satisfy the ANSI N545-1975 energy dependence requirement. More specifically, the main goal was to accomplish this using $CaSO_4$:Dy TL material in conjunction with a single energy compensating metal filter.

The response of $CaSO_4$:Dy to photons is very dependent on energy. This is due to the relatively high effective atomic number of $CaSO_4$:Dy compared to air. Photon interaction cross sections vary greatly with atomic number. This is especially true for energies below about 150 keV (0.15 MeV). For example, the mass energy absorption coefficient for 80 keV (0.08 MeV) photons is approximately four times greater for $CaSO_4$:Dy than for air. Since these coefficients are nearly the same for 1.25 MeV photons, an unfiltered $CaSO_4$:Dy dosimeter calibrated using a ^{60}Co source (average photon energy of 1.25 MeV) would overrespond to 0.08 MeV photons by a factor of four. Theoretically, if one were to use a filter that would remove 75% of 0.08 MeV photons while remaining transparent to 1.25 MeV photons, a filtered $CaSO_4$:Dy dosimeter calibrated to ^{60}Co would respond equally to 0.08 MeV and 1.25 MeV photons. The ideal filter would selectively filter out that fraction of all photon energies that is equal to the reciprocal of the ratios of

the mass energy absorption coefficients of $CaSO_4$:Dy and air for each energy. This method of compensating for energy dependence has been widely studied (Bacci and Bernabei 1981; Pradhan and Bhatt 1979).

1.5 Summary

Thus far, Chapter 1 has given an introduction to the background and the objective of this study. Chapter 2 will describe the materials and methods used. Section 2.1 contains a detailed description of the dosimeters used. This includes a description of the TL material. The terms "TL material" and "phosphor" are used interchangeably throughout this paper, always referring to $CaSO_4$:Dy. Details of the dimensions and physical composition of the TLDs are also included in this section.

The energy dependence of $CaSO_4$:Dy phosphor is calculated in Section 2.2. In Section 2.3, an analytical method was used to calculate photon transmission through each of the metal filters used in this study. The calculated transmissions are applied to the energy dependence calculations of the phosphor to estimate the energy dependence of the TLDs. Limitations of this approach that led to the use of the Monte Carlo method are also discussed.

Section 2.4 contains a general discussion of the EGS4 Monte Carlo code (Nelson et al. 1985), along with some details of the specific user code that was developed for this study. In Section 2.5 the rationale for interpreting the EGS4 output data is discussed.

The experimental method used to measure the energy dependence of the TLDs is given in Section 2.6. This includes details of the TLD preparation,

sources and methods of radiation exposure, dosimeter calibration, and phosphor readout.

Initial EGS4 simulations of dosimeters without metal filtration are presented in Section 2.7. Discrepancies between these calculations and the energy dependence calculations from Section 2.2 are discussed.

In Section 3.1, the results of the EGS4 simulations of dosimeters with metal filters are presented. Errors associated with the calculations and the experimental data are discussed in Section 3.2. This includes statistical uncertainties in the EGS4 calculations and both statistical and systematic uncertainties in the experimental results. Section 3.3 is a discussion of the discrepancies between the EGS4-calculated results and the measured data.

Section 4.1 is a summary of the study. Conclusions that can be drawn from the study are discussed in Section 4.2. Section 4.3 contains suggestions for further studies.

2. MATERIALS AND METHODS

2.1 Dosimeter description

Often the objective of environmental monitoring is to measure small changes in the natural radiation background level, typically around 100 milliroentgens (mR) per year. To achieve this objective requires a very sensitive radiation detector. The TL material used in this study was TLD-900 ($CaSO_4$:Dy), manufactured by Harshaw Chemical Co. It consists of $CaSO_4$ doped with 0.21% of dysprosium as the impurity. This phosphor is commonly used for environmental monitoring due to its high sensitivity. Radiation doses as low as 1 mR can be measured with a precision of ±15% at 1 standard deviation (Webb 1972).

The glow curve of $CaSO_4$:Dy shows a primary glow peak at approximately 220°C with many lesser peaks ranging from about 85°C to 510°C. The emission spectrum has a main peak at 425 nanometers (Horowitz 1984). The phosphor used in this study was annealed at 400°C for 1 hour.

Figs. 1 and 2 are conceptual drawings of the cadmium-filtered TLD and the two brass-filtered TLDs respectively. Thirty-five milligram aliquots of $CaSO_4$:Dy powder were dispensed into low-density polyethylene (LDPE) capsules. The cylindrical capsules, measuring 1.5 cm in length, had a 0.4 cm outer diameter with a 0.08 cm wall thickness. They were sealed at their open ends with nylon plugs. Each TLD consisted of two identical capsules loaded in tandem into a metal filter tube with an inner diameter just large enough to fit the capsule.

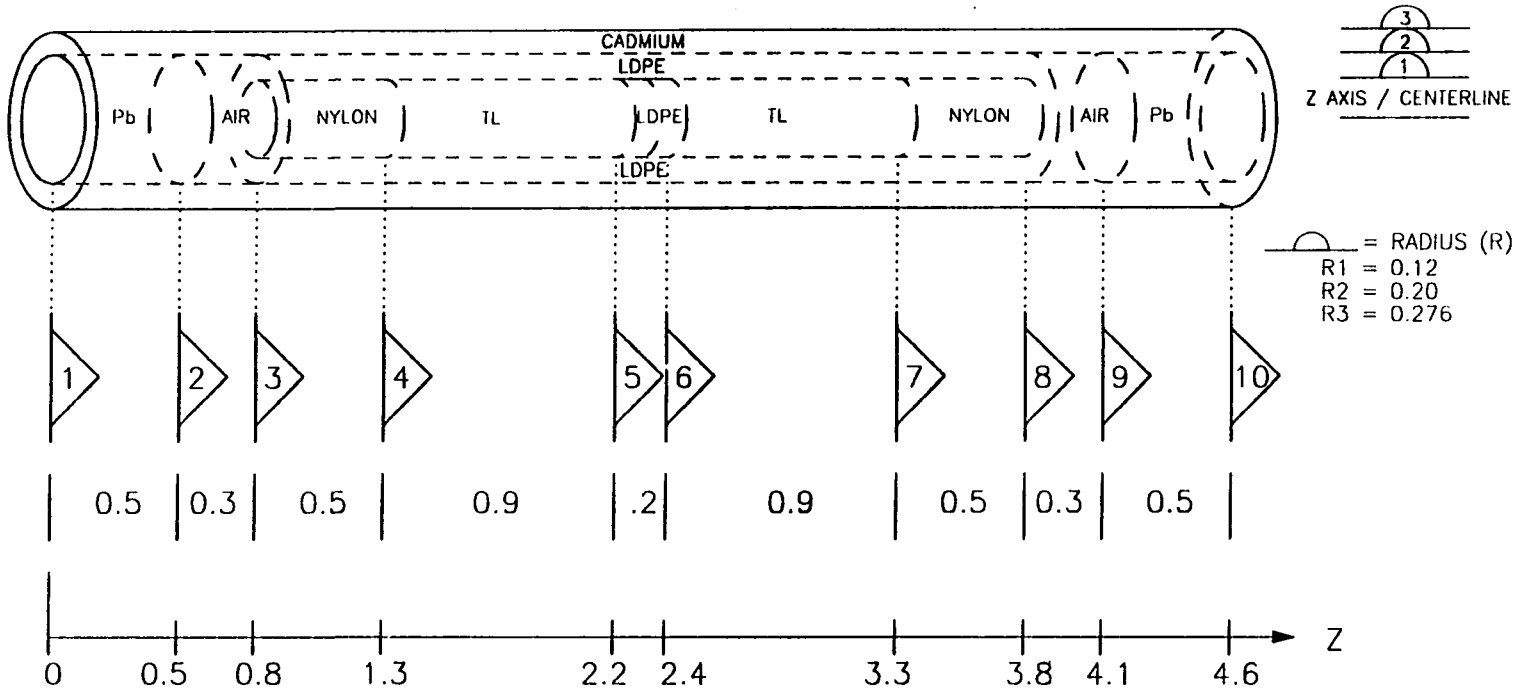

Fig. 1. Conceptual drawing of the dosimeter that utilized a cadmium energy compensation filter. Shown are duplicate low density polyethylene capsules (LDPE) containing $CaSO_4$:Dy TL matererial. The capsules are plugged at the open end with nylon and contained within a cadmium filter tube. The tube is sealed at the ends with lead. The "flags" represent cross-sectional planes. The "semi-circles" represent the radii (R1, R2, and R3) of the various dosimeter components about the cylindrical axis (Z). All units are given in centimeters.

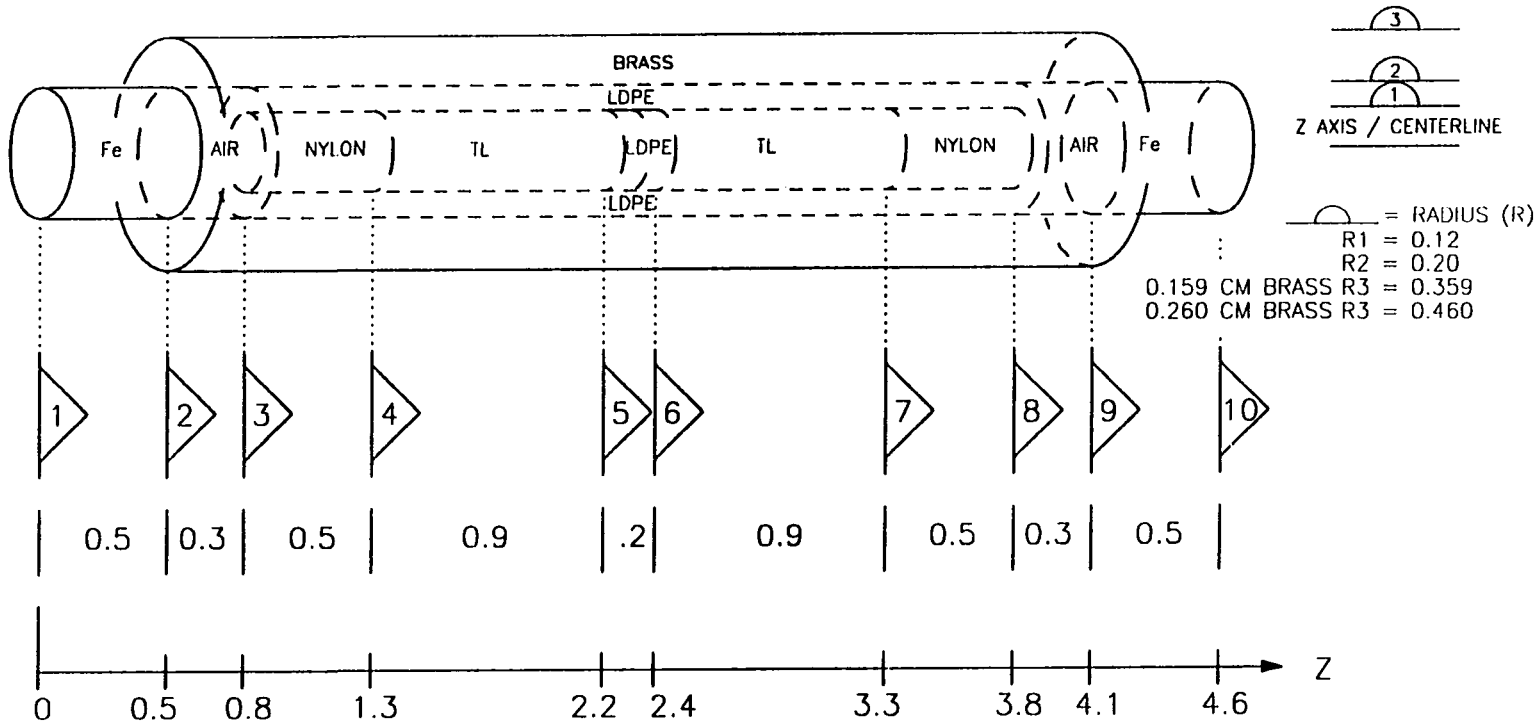

Fig. 2. Conceptual drawing of the dosimeter that utilized brass energy compensation filters. Shown are duplicate low density polyethylene capsules (LDPE) containing $CaSO_4$:Dy TL matererial. The capsules are plugged at the open end with nylon and contained within a brass filter tube. The tube is sealed at the ends with iron. The "flags" represent cross-sectional planes. The "semi-circles" represent the radii (R1, R2, and R3) of the various dosimeter components about the cylindrical axis (Z). All units are given in centimeters.

The ends of the metal filter tubes were plugged with either steel or lead, depending on filter type. For simplicity in the calculations, the steel plugs were assumed to consist of 100% iron (Fe). This assumption should have negligible effect on the results since the plugs are located at the ends of the dosimeters with the radiation being incident from the perpendicular direction. With the given geometry, the photon scattering effects from steel and iron may be assumed to be identical.

In Figs. 1 and 2, the TLDs are shown with the Z-axis as the cylindrical axis. The "flags" shown in the drawings represent semi-infinite cross-sectional planes, normal to the cylindrical axis. The spacing between the planes are given in units of centimeters. Also shown in the drawings are concentric cylinders centered about the Z-axis. These cylinders are located at the interfaces of the various dosimeter components and are symbolized in the figures by "semi-circles." The radii of the cylinders (R) are also given in units of centimeters. The planes and cylinders are used in the EGS4 code to divide the TLD into discrete regions.

Three different types of filter tubes were studied:

1) Cadmium, 0.076 cm: Cadmium tubes with lead solder plugs at each end (Fig. 1). The cadmium filter was actually constructed from 0.038 cm (15 mil) cadmium sheets rolled into tubes that were two layers thick.
2) Brass, 0.159 cm: Brass tubes, 0.159 cm wall thickness with iron shot plugs at each end (Fig. 2).

3) Brass, 0.260 cm: Brass tubes, 0.260 cm wall thickness with iron shot plugs at each end (Fig. 2).

The three filter types used in this study were selected mainly because of their availability. Also, the estimated dosimeter response calculations described in the following section suggested that the cadmium filter and the thicker brass filter would be good candidates for meeting the ANSI energy dependence requirement. Table 1 gives the physical description of the dosimeter components.

Table 1. Physical description of dosimeter components.

Media name	Elemental composition	Density (g/cm^3)
TL (phosphor)	$CaSO_4$: 0.21% Dy	2.61
Nylon	$(C_6H_{11}NO)_n$	1.14
Air	75.527% N, 23.178% O, 1.283% Ar, 0.012% C	0.001205
Lead	Pb	11.34
Low density polyethylene (LDPE)	$(C_2H_4)_n$	0.94
Cadmium	Cd	8.65
Brass	66.5% Cu, 33.0% Zn, 0.5% Pb	8.5
Iron	Fe	7.86

2.2 Energy dependence of bare $CaSO_4$:Dy

The photon energy dependence of TL materials is given by

$$S(E) = \frac{(\mu_{en}/\rho)_{CaSO_4:Dy}}{(\mu_{en}/\rho)_{air}}\eta(E) \qquad (1)$$

(Horowitz 1984) where S(E) is the energy-dependent relative TL response, assuming negligible self-absorption and the existence of electronic equilibrium. The parameter $(\mu_{en}/\rho)_{CaSO_4:Dy}$ is the mass energy absorption coefficient for $CaSO_4$:Dy and $(\mu_{en}/\rho)_{air}$ is the mass energy absorption coefficient for air. The variable $\eta(E)$ is the energy-dependent relative TL efficiency.

The reason for comparing the mass coefficient of $CaSO_4$:Dy to that of air is because radiation exposure is only defined for air. Environmental radiation measurements are typically measured by exposure and reported in units of roentgen or some other unit specific for ionization in air. The unit for exposure used throughout this paper is the roentgen (R) or milliroentgen (mR). The mass energy absorption coefficient is a measure of the average fractional amount of incident photon energy transferred to kinetic energy of charged particles in the medium.

The light output from a given TL material is dependent primarily on the total energy deposited within the material. In addition to the total energy deposited, the light output may also depend to some degree on the energy of the incident radiation. Ionization density effects due to variations in linear energy transfer (LET) as a function of incident photon energy and phosphor grain size have been postulated as contributing to this effect (Horowitz 1984).

This phenomenon is called the energy-dependent relative TL efficiency and is denoted by the symbol, $\eta(E)$ in Eq. (1). Since the available data for $\eta(E)$ is scarce and inconsistent for $CaSO_4$:Dy, it is assumed to be unity in all of the calculations (Bassi et al. 1976).

Table 2 lists the elemental composition of $CaSO_4$:Dy.

Table 2. Percent by weight elemental composition of $CaSO_4$:Dy.

Element	Fraction by Weight
Calcium	0.2937
Sulfur	0.2349
Oxygen	0.4689
Dysprosium	0.0021

The weighted averages of the mass coefficients for each element (Israel and Storm 1970) were used to determine the mass energy absorption coefficients of $CaSO_4$:Dy, as shown in Eq. (2).

$$(\mu_{en}/\rho)_{CaSO_4:Dy} = [(\mu_{en}/\rho)_{Ca} \times 0.2937] + [(\mu_{en}/\rho)_{S} \times 0.2349] + [(\mu_{en}/\rho)_{O} \times 0.4689] + [(\mu_{en}/\rho)_{Dy} \times 0.0021] \quad (2)$$

The mass energy absorption coefficients for air were taken directly from Appendix D3 of Attix (1986). The energy dependence of $CaSO_4$:Dy was calculated using Eq. (1) for photon energies between 0.01 and 1.5 MeV. Similar calculations have been made by Bassi et al. (1976). Fig. 3 shows the calculated energy dependence of bare $CaSO_4$:Dy. The over-response for energies below about 0.15 MeV is clearly seen, due to the high effective atomic

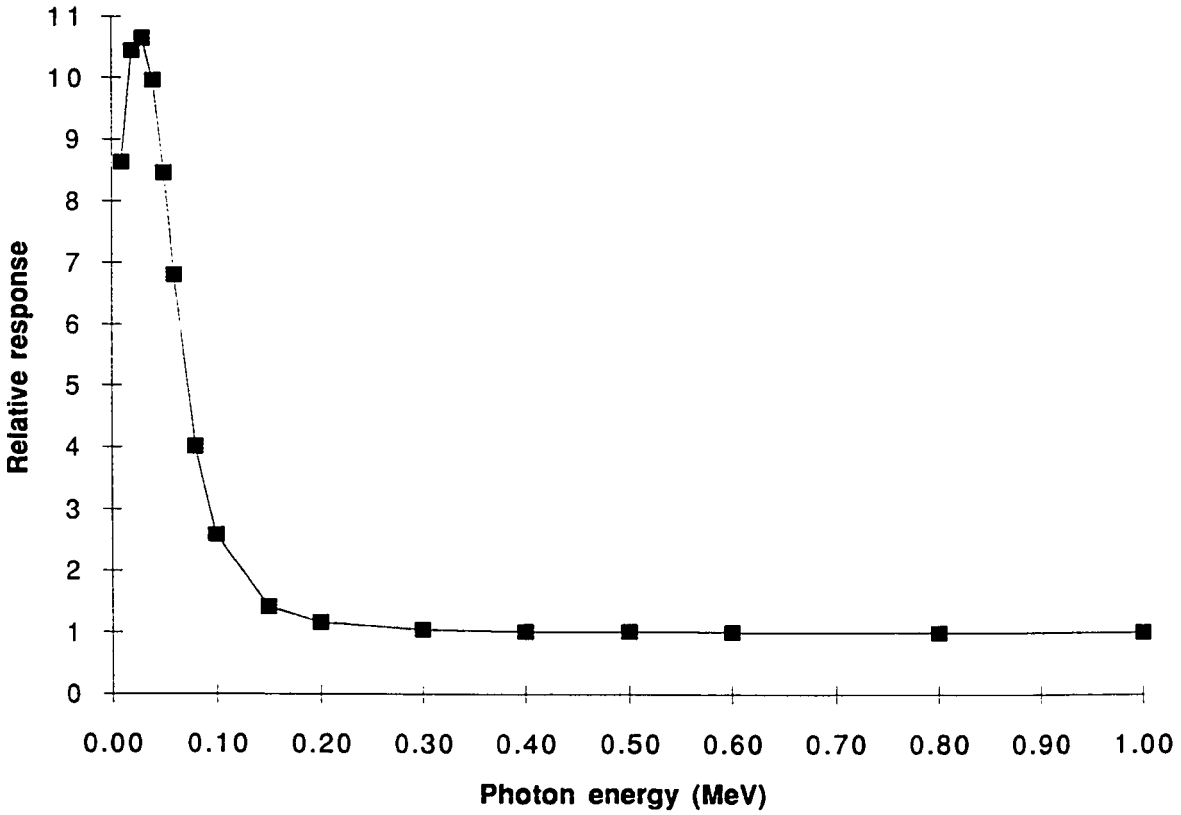

Fig. 3. Energy dependence of bare $CaSO_4$:Dy, calculated as the ratio of the mass energy absorption coefficients of $CaSO_4$:Dy and air. Notice the extreme energy dependence for energies below 0.15 MeV. The need for an energy compensation filter is clearly indicated, to avoid the over-response at the lower photon energies.

number of $CaSO_4$:Dy compared to air. Appendix A is a spreadsheet showing the steps taken to calculate the energy dependence data. The actual data used to generate Fig. 3 is listed in the last column of Appendix A. Note that the results of these initial $CaSO_4$:Dy energy dependence calculations will be used in the following section to estimate the dosimeter response using the analytical method.

2.3 Estimated dosimeter response

A simple approach was initially used to estimate the relative response of each dosimeter type. First, the photon transmission through each filter was calculated using linear attenuation as

$$\text{Transmission} = e^{-(\mu/\rho)(\rho)(x)} \tag{3}$$

where μ/ρ is the attenuation coefficient as a function of photon energy in cm^2/g, ρ is the density of the filter in g/cm^3, and x is the filter thickness in cm. The elemental composition (percent by weight) of the brass alloy and its density were given in Table 1. A weighted average of the attenuation coefficients for each element, similar to that given by Eq. (2), was used to determine the attenuation coefficient for brass. [Note that the attenuation coefficients used to calculate transmission are distinctly different from the mass energy absorption coefficients, μ_{en}/ρ, used in Eq. (2).] Attenuation coefficients for each element for energies ranging from 0.05 MeV to 1.50 MeV were taken from Israel and Storm (1970). Appendix B1 shows how the coefficients for cadmium at 0.07, 0.09, and 0.12 MeV were determined by graphical interpolation of the other available data. Appendices B2 and B3 are plots of photon transmission as a function of energy through the 0.159 cm

and 0.26 cm brass filters respectively. The photon transmissions through the brass filters for 0.07, 0.09, and 0.12 MeV were determined from these curves using graphical interpolation.

The calculated transmissions as a function of energy through the three filters are shown in Fig. 4 and the numerical values are tabulated in the columns denoted as "Transmission" in Appendices C1 through C3.

The photon transmission at each energy multiplied by the unfiltered $CaSO_4$:Dy response as calculated in the previous section gives the estimated dosimeter response. The dosimeter response was then normalized to the response to 1.25 MeV photons. Throughout this paper, the term "relative response" means the response normalized to the response to 1.25 MeV photons or in the case of the experimental data, it means the response normalized to the response to ^{60}Co. In Fig. 5, the estimated relative response of the three dosimeter types is plotted as a function of photon energy.

Also shown in Fig. 5 as dashed lines, is the acceptable response range defined in ANSI N545 (1975). It would appear from these analytical calculations that the TLD utilizing the 0.260 cm brass filter would meet the energy dependence criteria and the cadmium-filtered TLD would come very close while the 0.159 cm brass-filtered TLD clearly would not satisfy the requirement. A comparison of these calculations with the results of the experimental measurements (Section 3.1), however, revealed some significant differences.

These initial analytical dosimeter response calculations used two simplifying assumptions. The first assumption is that the phosphor is filtered by a semi-infinite plane as opposed to being encapsulated within a

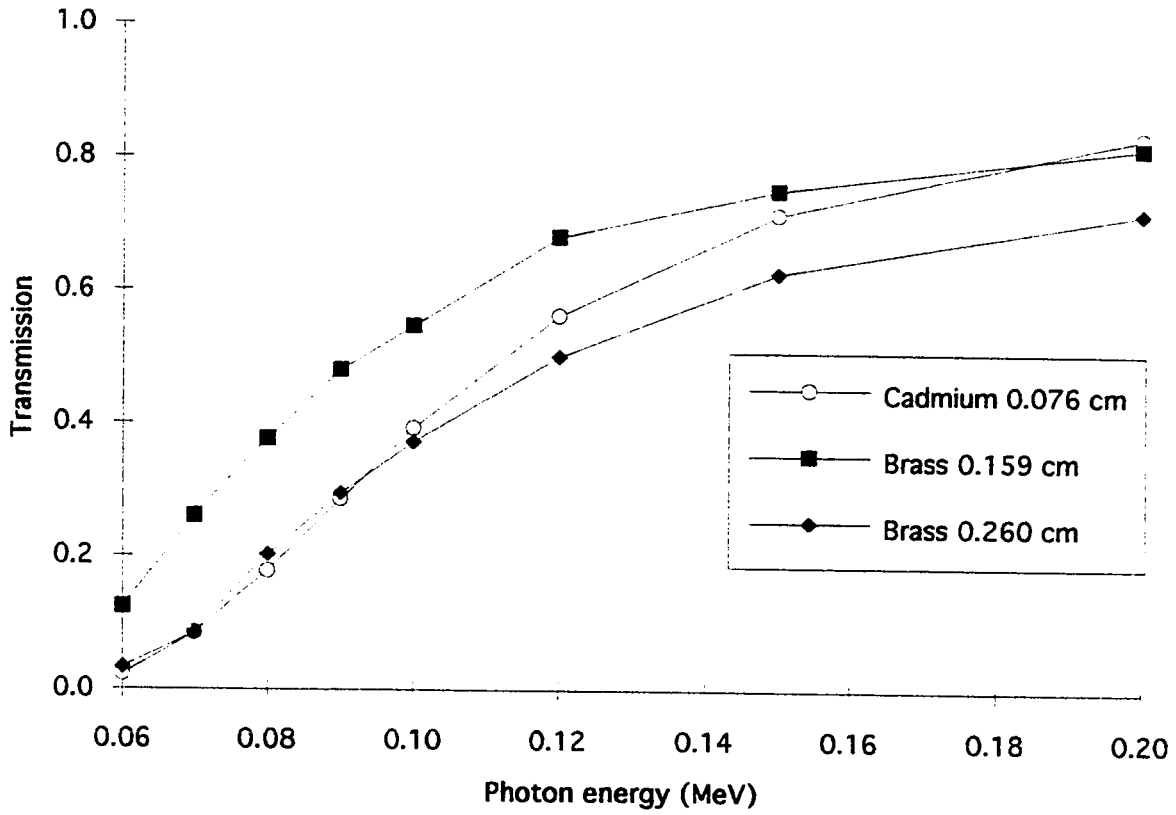

Fig. 4. Photon transmission as a function of energy through each of the three energy compensation filters, calculated using the analytical method. The ideal metal filter for use with $CaSO_4$:Dy would have a "transmission" that is equal to the reciprocal of the relative response of $CaSO_4$:Dy (Fig. 3) for all photon energies.

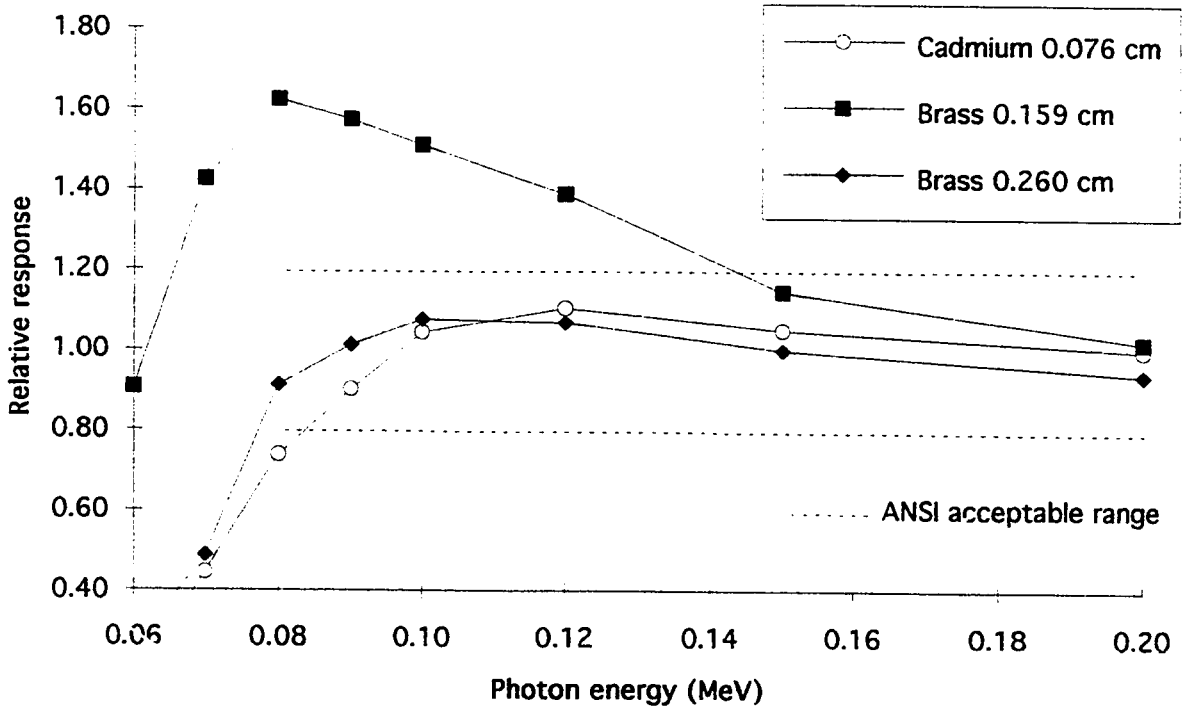

Fig. 5. Estimated dosimeter responses calculated using analytical methods for $CaSO_4$:Dy with three different energy compensation filters. It appears from these calculations that the relative response of the 0.260 cm brass-filtered TLD would satisfy the ANSI N545 energy dependence criteria (dashed lines) and that the cadmium-filtered TLD would come close. The experimental data (Section 3), however, clearly indicate that none of the TLDs meet the requirement.

cylindrical filter tube. Scattered photons from the cylinder walls are assumed to make no contribution to the dosimeter response. The second assumption is that the quality of the photon spectrum remained unaltered by the metal filter. Since $CaSO_4$:Dy is very energy dependent for photons below about 100 keV, the effects from scattered photons may be significant. A more rigorous energy response calculation method would consider both the dosimeter geometry and the effects from scattered photons. The Monte Carlo method was therefore selected to account for these other variables.

2.4 The EGS4 Monte Carlo code

The EGS4 Monte Carlo code used in this study was developed at the Stanford Linear Accelerator Center (Nelson et al. 1985). The Monte Carlo technique consists of using knowledge of the probabilities of individual interactions of photons and electrons with material to simulate the random trajectories of individual particles. The following photon and electron interaction processes are taken into account by the EGS4 Code:

Photoelectric effect

The photoelectric cross sections used by EGS4 are from Israel and Storm (1970). In all of the calculations, photoelectrons produced in $CaSO_4$:Dy, nylon, low density polyethylene, and air, are assumed to be emitted isotropically and any energy that is released in the form of K-edge x-rays is assumed to be deposited at the point of the interaction. The basis for this assumption is that the energies of the fluorescent x-rays are low for these media and would not be expected to travel any appreciable distance. For copper, cadmium, lead, and iron, the photoelectron angular distribution

was sampled (Blielajew and Rogers 1986) using Sauter's theory. Also, for these metals, K-edge fluorescent x-rays are further tracked. For comparison purposes, calculations were also made where the photoelectron angular distribution was not sampled in the metals. Auger electrons were not transported. Any energy released in the form of Auger electrons is deposited locally.

Compton scattering

The Compton scattering cross sections are calculated using the formulas by Klein and Nishina (1929).

Pair production

This process is not energetically possible for most of the photon energies considered in this work, although it is accounted for using formulas from Motz et al. (1969).

Bremsstrahlung

Bremsstrahlung processes are accounted for using formulas from Koch and Motz (1959).

Multiple scattering

This refers to elastic collisions of electrons with atomic nuclei, whereby electrons change direction without significantly losing energy. For these scattering processes, Molière's (1948) theory is used.

Continuous energy loss of electrons

Total stopping power consists of soft bremsstrahlung and collision loss terms. Collision loss is determined by the (restricted) Bethe-Bloch stopping power with Sternheimer treatment of the density effect.

Rayleigh scattering

There is no transfer of energy with Rayleigh scattering. Also, with the given geometry of the TLDs, an equal number of photons would be expected to be scattered into the TL regions as scattered away from the TL regions. For these reasons, the Rayleigh scattering routine was not included, as it would only add computing time and would not significantly affect the results.

Following any of the above interactions, the trajectories and energies of each of the resulting photons and electrons are calculated and tracked. Large numbers of individual simulations provide information on average physical quantities. In this work, approximately 500,000 to 1,000,000 individual source photons were transported for each data point; the physical quantity of primary interest was the energy deposited in the phosphor.

In order to use the EGS4 code the user must write a "User Code" which consists of a MAIN program and subroutines HOWFAR and AUSGAB. The MAIN program performs any initialization needed for the other subroutines. It contains such things as the names of the media to be used and specifies the geometry parameters such as distance units. Detailed information about the media (Table 1) is loaded into the EGS4 companion code, PEGS4, which in turn prepares the necessary interaction cross sections that are used in the simulations. Cross sections were prepared in PEGS4 for all media for electron energies ranging from 0.521 MeV (kinetic energy of 0.01 MeV), designated as "AE", to 10.511 MeV (kinetic energy of 10 MeV), designated as "UE". Photon

cross sections for the media were prepared in the range from 0.001 MeV (AP) to 10 MeV (UP).

The desired transport cutoff energies are also described in the MAIN program. For the simulations in this work, electrons were tracked until they reached a kinetic energy of 0.01 MeV (ECUT), and photons were tracked until they reached 0.001 MeV (PCUT), at which point their energies were deposited locally.

The geometry of the dosimeter is described in subroutine HOWFAR. Figs. 1 and 2 are conceptual drawings of the dosimeters. Figs. 6 and 7 show the corresponding simulated geometry as described in the HOWFAR subroutine. For this work, the geometry is described as four concentric cylinders centered about the Z-axis. These cylinders are subdivided by ten semi-infinite planes. The numbers of slabs and cylinders are given in MAIN, along with their respective dimensions. In this manner, all components of the dosimeter are separated into discrete identifiable regions. The regions being solid rings (or solid cylinders as is the case with the innermost regions) centered about the Z-axis. The physical characteristics and dimensions of each region are defined in MAIN. Region 1, although not indicated in Figs. 6 and 7, is the entire region on the negative Z side of the X-Y plane. Region 1, along with regions 11, 21, and 31 through 41 are referred to as discard regions. Particles entering discard regions are exiting the dosimeter system in an "outward" direction and are no longer tracked by the EGS4 program. For the brass-filtered dosimeters (Fig. 7), regions 22 and 30 are also discard regions.

Notice in Figs. 6 and 7 that regions 5 and 7 contain the TL material. With the scoring subroutine AUSGAB, the user has the capability of defining

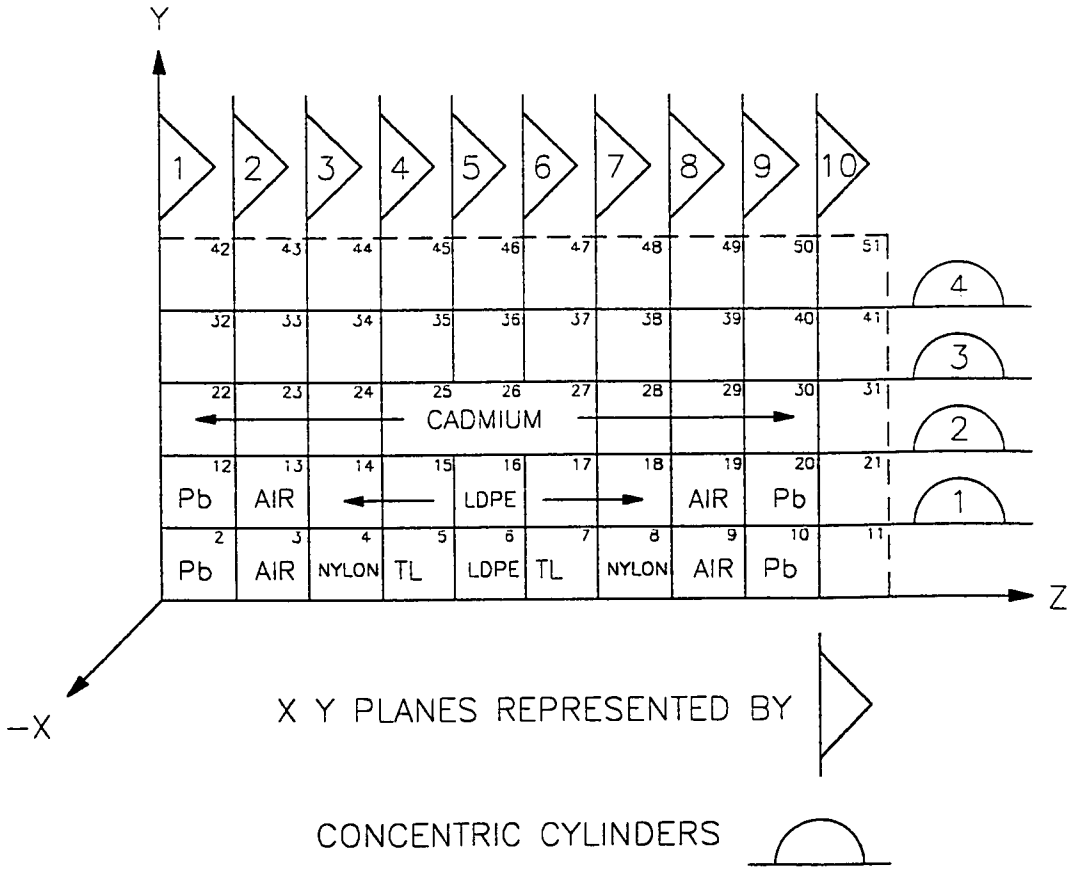

Fig. 6. EGS4 simulated geometry for the cadmium filtered dosimeter as described in the HOWFAR subroutine. The planes and concentric cylinders centered about the Z-axis divide the TLD into discrete regions. Source photons are incident from the positive Y direction. Notice that regions 5 & 7 are the TL regions. The average fraction of energy [f(E)] deposited in the TL regions is the value that is used in Eq. (8) to calculate the relative TLD response.

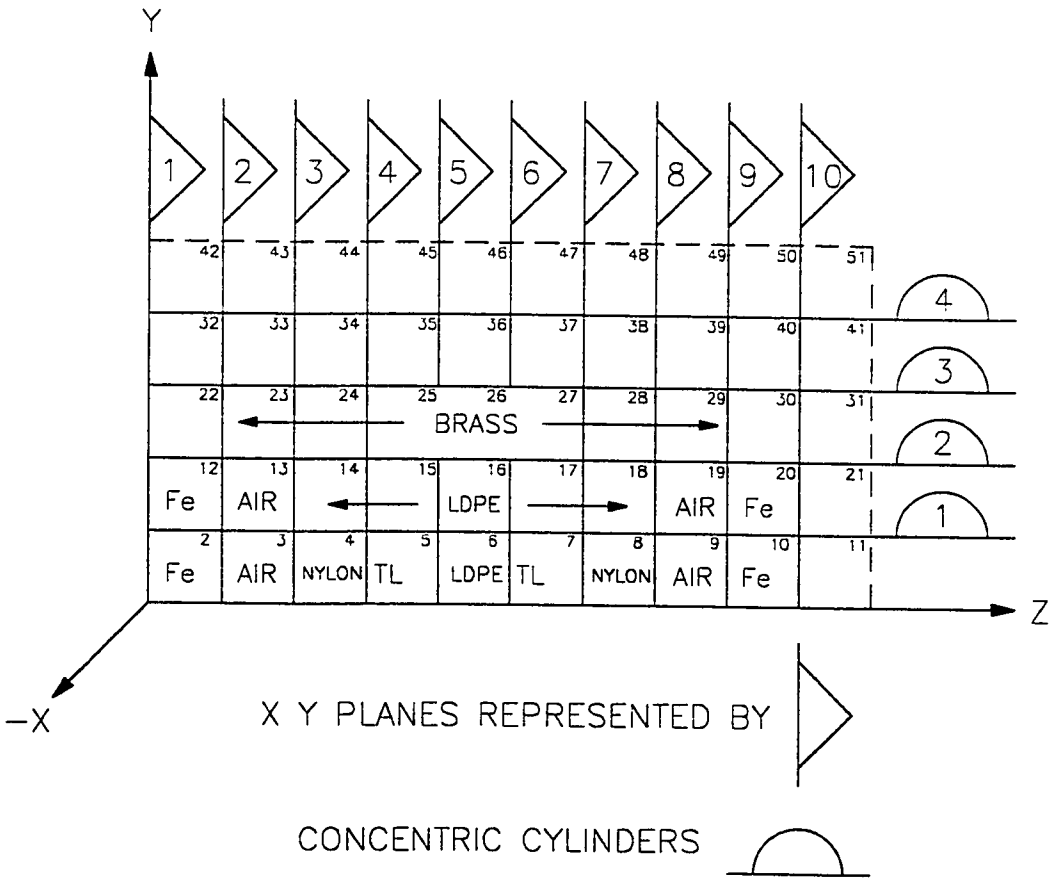

Fig. 7. EGS4 simulated geometry for the brass filtered dosimeters as described in the HOWFAR subroutine. The planes and concentric cylinders centered about the Z-axis divide the TLD into discrete regions. Source photons are incident from the positive Y direction. Notice that regions 5 & 7 are the TL regions. The average fraction of energy [f(E)] deposited in the TL regions is the value that is used in Eq. (8) to calculate the relative TLD response.

the output from any set of simulations. For example, the user may wish to keep track of Compton scattering events or photoelectric events, etc., in anynumber of regions. In this work, the primary parameter of interest is the fraction of the total energy that is incident on the dosimeter which is deposited in regions 5 and 7, the TL regions.

A description of the incident particle is given in MAIN. For this study they were photons with energies ranging from 0.01 to 1.25 MeV. The photons were randomly incident on the dosimeter from a single direction perpendicular to the cylindrical axis, thus simulating a uniform radiation field. In the geometry subroutine, HOWFAR, the Z-axis is the cylindrical axis. The XYZ coordinates of the incident photon were randomly selected using a random number generator as

$$\begin{aligned} Z &= L \times ranz \\ X &= r - (ranx \times 2r) \\ Y &= \sqrt{r^2 - x^2} \end{aligned} \tag{3}$$

L = the length of the dosimeter (from plane 1 to plane 10, Figs. 6&7)

ranz = a random number between 0 and 1

r = the outer radius of the dosimeter (radius of cylinder 3, Figs. 6&7)

ranx = a random number between 0 and 1 (independent of ranz).

Since the experimental data was obtained by exposing dosimeters to two x-ray spectra, M150 and H150 (ANSI 1993), as opposed to monoenergetic photons, x-ray spectra were also simulated. This was accomplished by using the rejection technique. One random number was used to select a photon energy, with all possible photon energies in the spectrum having equal

probability of selection. A second random number was used to either accept or reject the photon energy selected depending on its intensity in the spectrum. A comparison of the sampled spectra to the actual spectra as supplied by Battelle Pacific Northwest Laboratories (PNL) is shown in Figs. 8 and 9. The agreement between the measured and simulated spectra confirms that the sampling scheme using the rejection technique works successfully.

2.5 Rationale for interpreting EGS4 output data

The primary objective of the EGS4 simulations is to calculate the relative photon energy dependence of various types of dosimeters. The TLD response is proportional to the total energy deposited in the TL material. This relationship is given by

$$\text{TLD Response} \quad \propto \quad f(E)\,\phi\,E\,\eta(E) \tag{4}$$

where

$f(E)$ = average fraction of energy deposited in regions 5 and 7, the TL regions, for any given energy. (This value is obtained from the EGS4 output.)

ϕ = photon fluence

E = incident photon energy

$\eta(E)$ = energy-dependent relative TL efficiency, assumed to equal 1 in these calculations.

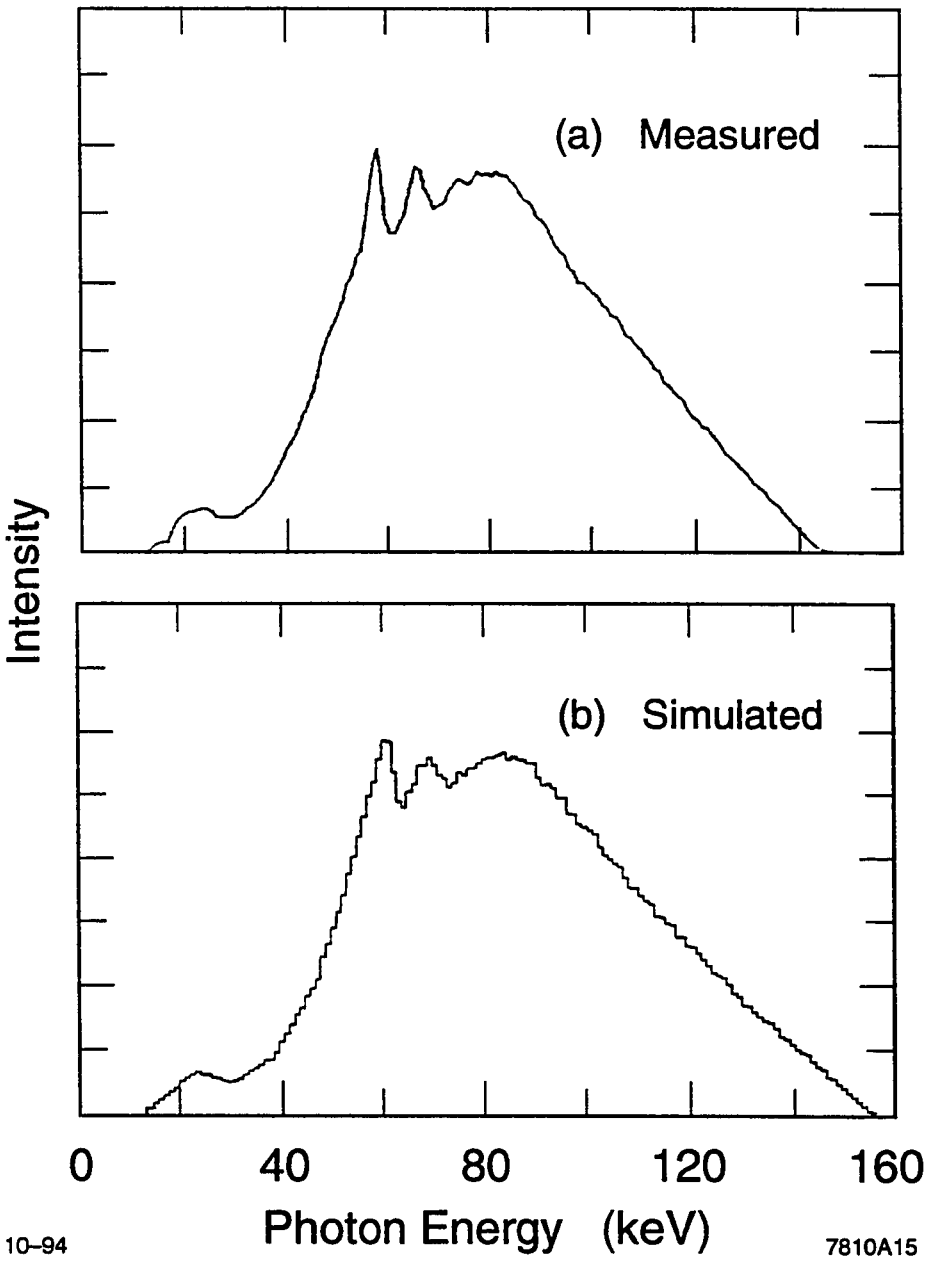

Fig. 8. Measured M150 x-ray spectrum, data supplied by PNL (top) compared with the EGS4 simulated M150 x-ray spectrum (bottom). The average energy for this spectrum is reported by PNL to be 0.07 MeV. The agreement between the measured and simulated spectra confirms that the rejection technique used to sample the x-ray spectrum was successful.

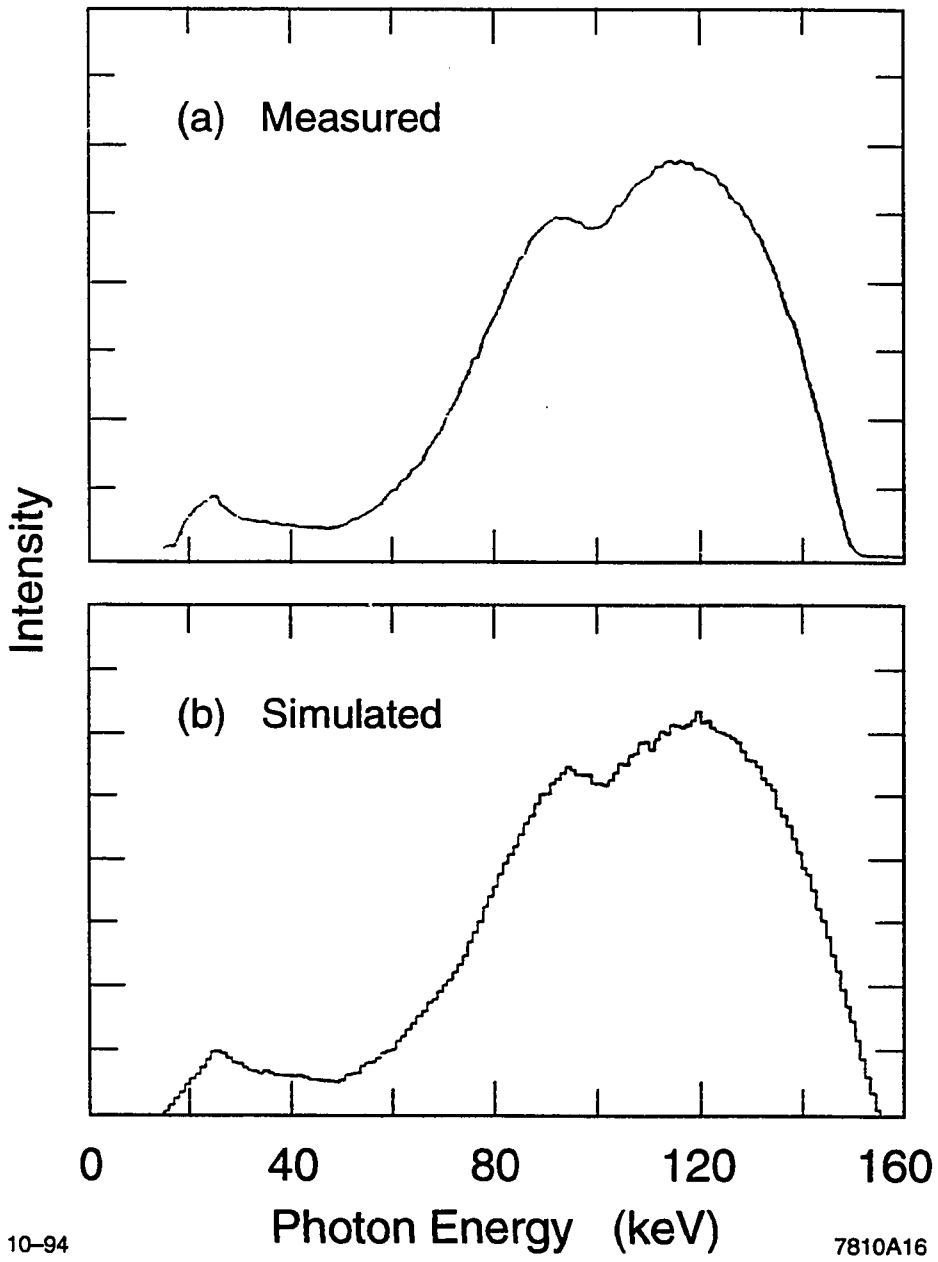

Fig. 9. Measured H150 x-ray spectrum, data supplied by PNL (top) compared with the EGS4 simulated H150 x-ray spectrum (bottom). The average energy for this spectrum is reported by PNL to be 0.12 MeV. The agreement between the measured and simulated spectra confirms that the rejection technique used to sample the x-ray spectrum was successful.

Radiation exposure is proportional to the photon fluence, photon energy, and the mass energy absorption coefficient for air:

$$\text{Exposure} \quad \propto \quad E\,\phi(\mu_{en}/\rho)_{air(E)} \tag{5}$$

where

$(\mu_{en}/\rho)_{air(E)}$ = the mass energy absorption coefficient for air as a function of the incident photon energy.

Combining Eq. (4) and Eq. (5) gives

$$\frac{\text{TLD Response}}{\text{Exposure}} \propto \frac{f(E)\phi E}{E\phi(\mu_{en}/\rho)_{air(E)}} \tag{6}$$

which reduces to

$$\frac{\text{TLD Response}}{\text{Exposure}} \propto \frac{f(E)}{(\mu_{en}/\rho)_{air(E)}} \tag{7}$$

and normalizing to 1.25 MeV gives

$$\text{Relative TLD Response} = \frac{\left(\dfrac{f(E)}{(\mu_{en}/\rho)_{air(E)}}\right)}{\left(\dfrac{f(1.25\ \text{MeV})}{(\mu_{en}/\rho)_{air(1.25\ \text{MeV})}}\right)} \tag{8}$$

From the above expression, the f(E) values from the EGS4 calculations can be used to obtain the relative energy dependence of various types of dosimeters with the results normalized to 1.25 MeV.

The mass energy absorption coefficients $[(\mu_{en}/\rho)_{air}]$ for the x-ray spectra, M150 and H150, were assumed to be equal to the coefficients of their corresponding average photon energies, 0.070 and 0.120 MeV. The values for $(\mu_{en}/\rho)_{air}$ for 0.070 and 0.120 MeV are 0.0274 and 0.0240 cm^2/g, respectively.

2.6 Experimental method

The experimental dosimeters were prepared and analyzed at Radiation Detection Company (RDC), Sunnyvale, California.

For the energy range considered, 0.08 to 1.5 MeV, the over-response of $CaSO_4$:Dy is most significant for energies below about 0.15 MeV. Unfortunately, monoenergetic photon sources with energies between 0.08 and 0.15 MeV and with source strengths capable of delivering useful dose rates are not common and were unavailable for this work. Instead, two x-ray sources, with beam codes M150 and H150, with average photon energies of 0.07 and 0.12 MeV respectively, were used as the radiation sources for the measurements. The x-ray irradiations were made at Battelle Pacific Northwest Laboratories (PNL). Dosimeters were exposed free-in-air (no phantom). The delivered exposure was measured at PNL using an ion chamber.

Each exposure was 100 milliroentgens (mR). On the same day that the x-ray exposures were made at PNL, the calibration dosimeters were exposed to 100 mR from a ^{60}Co source at RDC. Since the calibration dosimeters were readout together with the dosimeters exposed to the x-ray spectra, fade corrections were unnecessary. The calibration dosimeter exposures were also made free-in-air. The exposure time for the calibration dosimeters was 11

minutes and 37 seconds at a distance of 1 meter. Control dosimeters were also included with each shipment to account for any transit doses.

The dosimeters were read on a Teledyne Model 7300 TLD reader. This is a manual TLD reader that utilizes a nitroger gas purging system. The planchet used to contain the $CaSO_4$:Dy contents of each polyethylene capsule was heated resistively. The heating ramp rate was 20°C per second to a maximum temperature of 260°C. The dwell time at 260°C was 10 seconds. The output signal from the reader, which is proportional to the light output from the phosphor and the exposure received by the dosimeter, is given in units of nanocoulombs (nC). The dark current ("empty planchet" reading) was 0.05 nC. The calibration as determined from the dosimeters exposed to 100 mR from ^{60}Co was 2.62 mR/nC. The average signal from the transit dosimeters ("mail controls") was 2.47 nC, which is equivalent to 6 mR.

2.7 EGS4 simulations of dosimeters without filtration

For the first set of Monte Carlo simulations, photons were incident on the "bare" dosimeter capsules without any metal filtration. This was an attempt to use EGS4 to calculate the energy dependence of $CaSO_4$:Dy by itself without filtration. It was also a check of the program to see if its calculated results seemed reasonable. The results are tabulated in Appendix D, showing the fractional energy deposition in the TL regions (regions 5&7) and the calculated relative response in the last column.

A comparison of this data with the energy dependence calculations in Section 2.2 (Appendix A) revealed some discrepancies. One discrepancy is that the EGS4 relative response calculations appear to be elevated for energies

below 1.25 MeV. This is likely to be due to a lack of charged particle equilibrium (CPE) in the simulated geometry for energies of 0.5 MeV and above. The analytical calculations in Section 2.2 assume CPE conditions for all photon energies. Since the LDPE capsule walls are not thick enough to provide CPE for all photon energies, particularly for 1.25 MeV, this assumption is not valid. The EGS4 code does not assume CPE. Since the EGS4-calculated relative responses are normalized to 1.25 MeV, it follows that the relative responses for the lower energies, where CPE conditions do exist, would be elevated compared with the analytical calculataions.

Another somewhat different discrepancy occurred at energies of 0.03 MeV and below. The relative dosimeter responses calculated from the EGS4 simulations are much lower than the previously calculated responses. This discrepancy may be attributed to the relatively high density of $CaSO_4$:Dy. Attenuation by the phosphor itself is significant at the lower energies. If the TL regions are not uniformly exposed, the dosimeter will underestimate the dose.

In general, the discrepancies appear to be geometry related. For the filtered dosimeter simulations, the dosimeter core is enveloped by metal of more than adequate thickness to provide CPE. Furthermore, the energies of concern are high enough that self-attenuation by the TL material is unlikely to significantly affect the results. This potential problem is discussed further in Section 3.3.

3. RESULTS AND DISCUSSION

3.1 EGS4 simulations of dosimeters with metal filters

The results of the EGS4 calculations given in Figs. 10, 11, and 12, are for dosimeters with filters consisting of 0.076 cm cadmium, 0.159 cm brass, and 0.260 cm brass, respectively. The data used to generate these plots are given in Appendices E1 (Fig. 10), E2 (Fig. 11), and E3 (Fig. 12). These data tables contain the EGS4 output for energy deposition in the TL regions (regions 5&7), labeled as "Fractional energy deposited" and the calculated "Relative response," last column. Also shown for comparison in Figs. 10, 11, and 12 are the "measured" data points (referring to the experimental method discussed in Section 2.6).

In all cases, the results of the EGS4 calculations are in closer agreement with the experimental results than were the analytical calculations of Section 2.3 (Fig. 5). Similar to the analytical calculations (Fig. 5), the EGS4-calculated response for the 0.260 cm brass-filtered dosimeter (Fig. 12) also appears to very nearly satisfy the ANSI N-545 energy dependence requirement. However, the experimental data clearly indicates that the dosimeter responses to M150 and H150 x-rays are not within the ANSI acceptable range for any of the dosimeters studied.

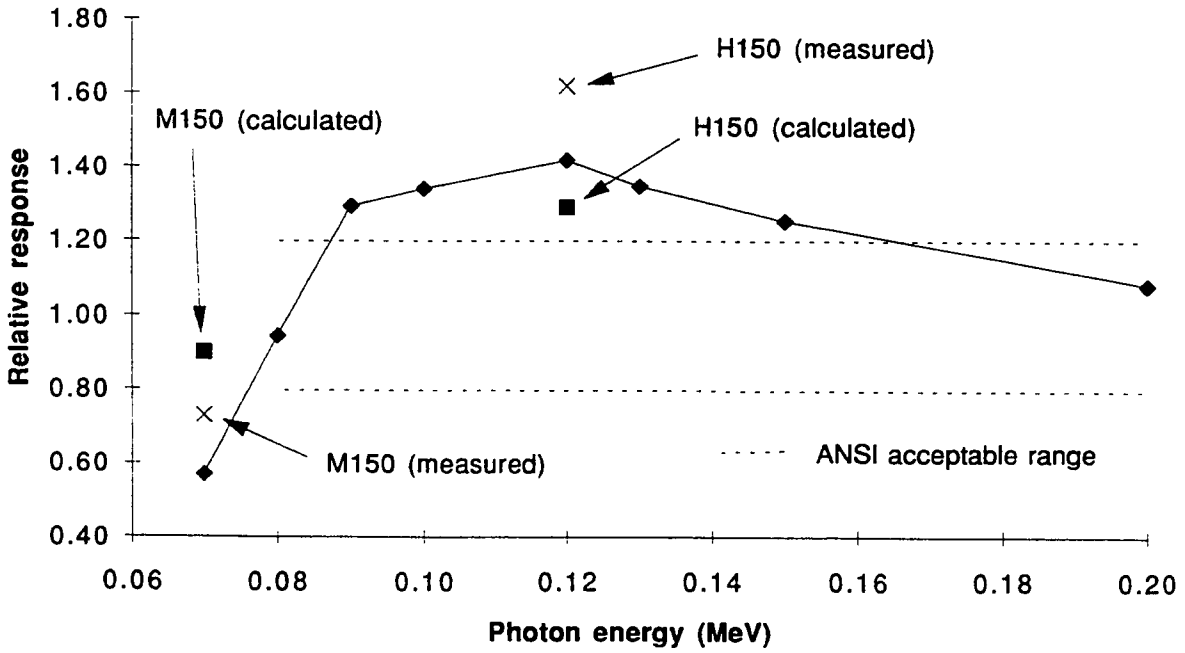

Fig. 10. EGS4 calculated energy response of dosimeter utilizing 0.076 cm thick cadmium filter to monoenergetic photons (solid line). Also shown is the EGS4 calculated responses and experimentally measured responses to M150 and H150 x-ray sources.

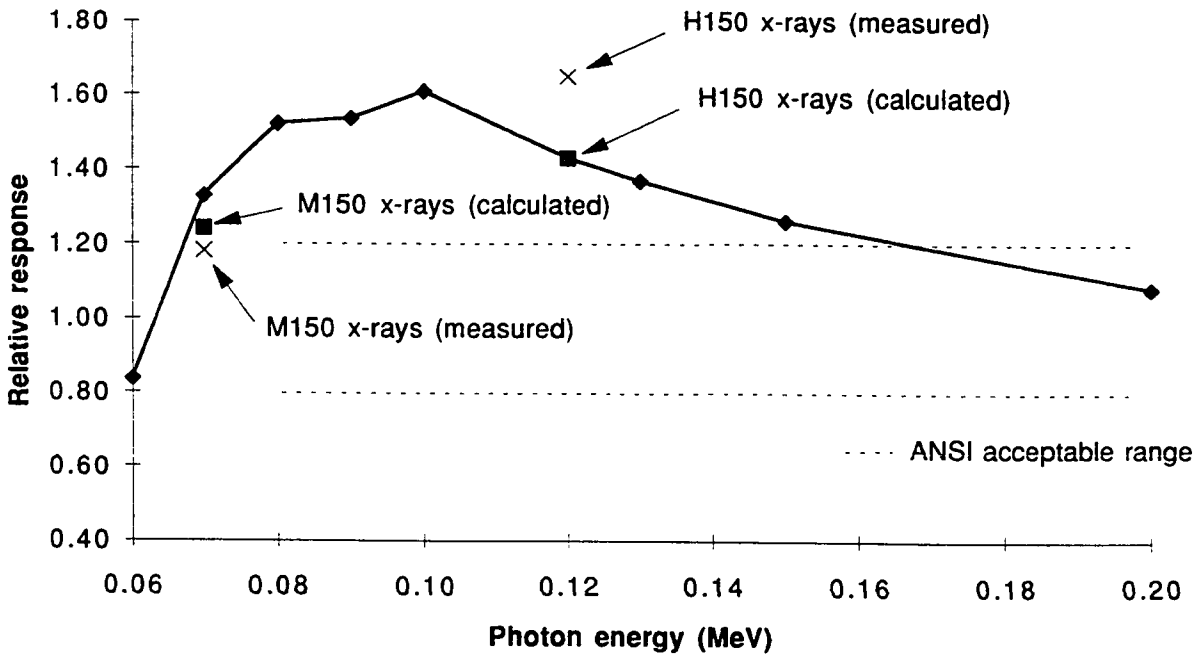

Fig. 11. EGS4 calculated energy response of dosimeter utilizing 0.159 cm thick brass filter to monoenergetic photons (solid line). Also shown is the EGS4 calculated responses and experimentally measured responses to M150 and H150 x-ray sources.

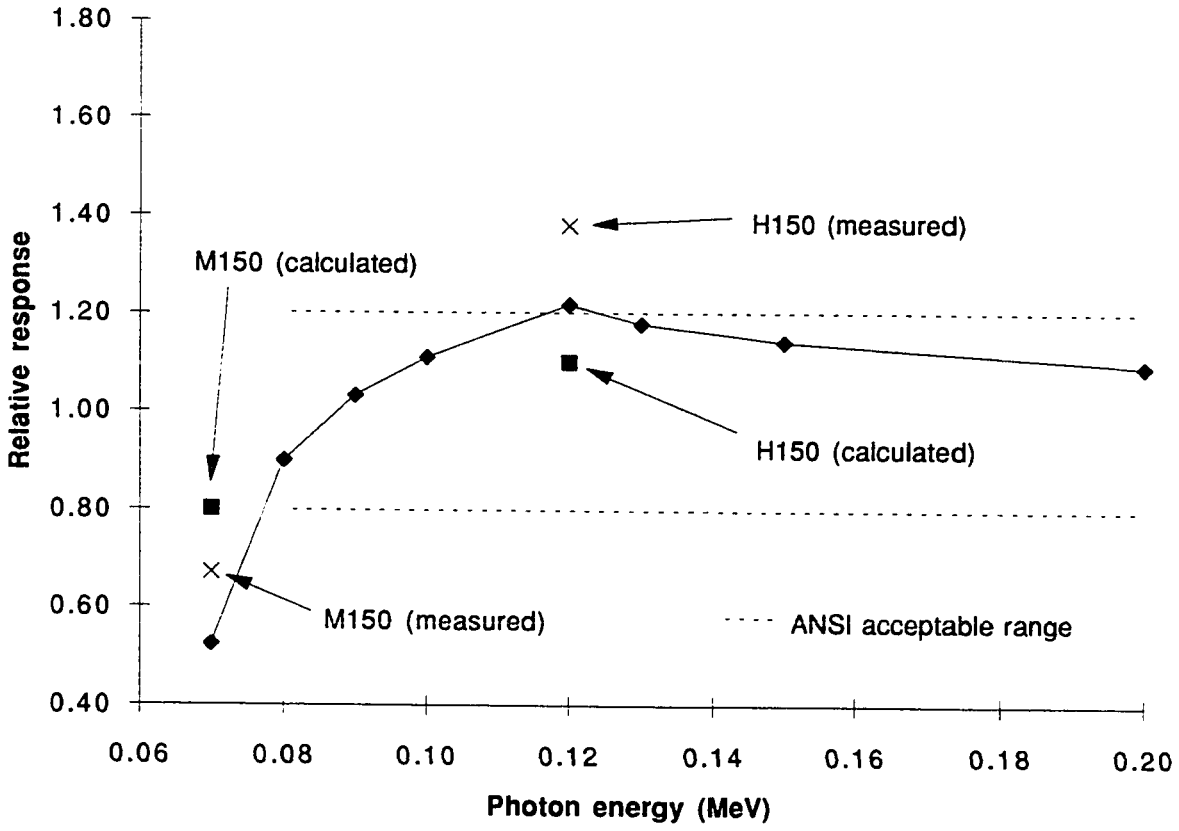

Fig. 12. EGS4 calculated energy response of dosimeter utilizing 0.260 cm thick brass filter to monoenergetic photons (solid line). Also shown is the EGS4 calculated responses and experimentally measured responses to M150 and H150 x-ray sources.

3.2 Error analysis

The statistical uncertainties associated with the EGS4 calculations were estimated by comparing results from two duplicate simulations or "runs." The last random number used for the initial run was used as the "seed" for a second otherwise identical run. The standard deviation was less than 3% for each of the duplicate runs. See Tables 3 and 4 below.

Table 3. Statistical uncertainty for EGS4 calculations for M150 x-rays.

Filter description		Average fraction of energy deposited in regions 5 & 7		Average	Standard
Material	Thickness	First run	Second run	(both runs)	deviation
Cadmium	0.076 cm	0.001003	0.0009672	0.0009851	2.6%
Brass	0.159 cm	0.001078	0.001086	0.001082	0.5%
Brass	0.260 cm	0.0005287	0.0005318	0.00053025	0.4%

Table 4. Statistical uncertainty for EGS4 calculations for H150 x-rays.

Filter description		Average fraction of energy deposited in regions 5 & 7		Average	Standard
Material	Thickness	First run	Second run	(both runs)	deviation
Cadmium	0.076 cm	0.001253	0.001246	0.0012495	0.4%
Brass	0.159 cm	0.001084	0.001061	0.0010725	1.5%
Brass	0.260 cm	0.0006365	0.0006167	0.0006266	2.2%

Both systematic and statistical uncertainties were considered in estimating the errors associated with the experimental data. Errors in exposing the calibration dosimeters such as source strength uncertainty, source to dosimeter distance, and time of exposure were considered. Other factors that contributed to experimental error include readout variability in duplicate TLD's exposed simultaneously to the x-ray sources, variability in background dosimeters that were used to determine calibration factors, calibration dosimeters, and control dosimeters. Table 5 gives the EGS4 "calculated" dosimeter responses, and the "measured" (experimental) dosimeter responses to M150 and H150 x-ray sources, along with their corresponding uncertainties. Notice that the differences between the calculated and measured values are generally greater than what can be accounted for from the estimated uncertainties.

Table 5. EGS4 dosimeter response calculations compared to experimentally measured dosimeter responses.

Filter description		Relative response M150 x-rays		Relative response H150 x-rays	
Material	Thickness	Calculated	Measured	Calculated	Measured
Cadmium	0.076 cm	0.90±0.05	0.73±0.09	1.29±0.06	1.62±0.08
Brass	0.159 cm	1.24±0.07	1.18±0.05	1.43±0.02	1.65±0.06
Brass	0.260 cm	0.80±0.04	0.67±0.03	1.10±0.05	1.38±0.07

3.3 Discussion of discrepancies

Note that in Figs. 10, 11, and 12 that the measured response is higher than the calculated response for H150 x-rays and lower than the calculated response for M150 x-rays. This suggests that something other than statistical errors are responsible for the discrepancies. Five possible causes were considered to explain the inconsistencies.

The first possible cause is that the simulated dosimeter volume may have been too large (radius equal to 0.12 cm) and that photons on the lower end of the energy spectrum were not capable of uniformly exposing the volume. To test this theory using EGS4, the radius of the TL volume was reduced from 0.12 cm to 0.05 cm. Subsequent simulations produced results that were not statistically different from those obtained previously.

The second potential cause is due to the way EGS4 simulates K-edge fluorescent x-rays following photoelectric events. Prior to adding the fluorescent x-ray transport routine to the EGS4 user code, fluorescent x-rays were assumed to be deposited locally. Appendices F1, F2, and F3 contain output data from early simulations that did not utilize the fluorescent x-ray transport routines. A comparison of this data with the corresponding data from Appendices E1, E2, and E3 (data used to create Figs. 10 through 12) , where K-edge fluorescent x-rays were tracked for cadmium, copper, lead, and iron, reveals significant differences, especially with the cadmium-filtered dosimeter. These differences are believed to be due to the treatment of fluorescent x-rays, which are relatively energetic for the metals, especially for cadmium. For the low Z dosimeter materials, nylon and polyethylene, and for the TL regions, the EGS4 routine for transporting fluorescent x-rays was

not used. Since the fluorescent x-ray energies for the low Z materials are low and their ranges are small relative to the sizes of the defined regions, the assumption that the x-ray energy is deposited locally in the non-metal media should be valid for the purposes of this work. It is conceivable, however, that following photoelectric events within the TL regions, a small fraction of energy in the form of fluorescent x-rays may actually escape the TL regions and be erroneously deposited in the TL regions by EGS4. This possibility could only result in EGS4 calculations that are erroneously high. This would certainly not explain why the calculated values were low compared to the experimental results for dosimeters exposed to H150 x-rays.

A third potential cause relates to the photoelectron angular sampling routine for the low Z materials and for the TL regions, where photoelectrons were always assumed to be emitted isotropically by EGS4. Since the TL regions are completely surrounded by polyethylene, the assumption of isotropic photoelectron emission should be a good one. To illustrate the validity of this assumption, consider the consequences of a hypothetical situation where photoelectrons are always emitted in the forward direction. The density of photoelectric events in the TL regions and in the immediate surrounding regions is constant. By assuming isotropic emission, photoelectrons on the incident photon side of the dosimeter that would erroneously be transported in the backward direction would never reach the TL regions. However, the same events when occurring on the opposite side of the dosimeter would erroneously be transported into the TL regions. The two errors would tend to cancel each other. This same argument could also be made for the surrounding metal filtration materials. Indeed, simulations

of the brass-filtered dosimeters were made in which photoelectron angular sampling was not used in the brass. These data are given in Appendices G1 and G2. The results differ only slightly from the corresponding data in Appendices E2 and E3, where photoelectron angular sampling was used.

It is difficult to explain the discrepancies between the calculations and the experimental data by only considering the potential errors associated with the EGS4 simulations. The discrepancies are too large and the EGS4 code has proven itself over the years to be successfull and reliable in numerous calculations involving photon-electron problems.

A fourth recognized potential source of error in the EGS4 calculations is the values used for $(\mu_{en}/\rho)_{air}$ for the x-ray spectra. It is likely that the actual $(\mu_{en}/\rho)_{air}$ values for the spectra are higher than the values used. Instead of simply assuming the values of $(\mu_{en}/\rho)_{air}$ for the x-ray spectra, M150 and H150, to equal the coefficients of their corresponding average photon energies, 0.070 and 0.120 MeV, an attempt to more accurately evaluate the effective $(\mu_{en}/\rho)_{air}$ for each x-ray spectrum was originally made. This involved taking a weighted average of the $(\mu_{en}/\rho)_{air}$ for all possible photon energies from 0 to 0.16 MeV at intervals of 0.01 MeV. The contributing $(\mu_{en}/\rho)_{air}$ for each photon energy was weighted depending on its intensity in the spectrum. The results of these evaluations were $(\mu_{en}/\rho)_{air}$ values that were 32% and 46% higher than the respective values for 0.07 and 0.12 MeV photons. It was found that the calculated values were extremely dependent on the estimated intensity of the 0.02 MeV point. Although this energy point only accounts for about 1.5% of the total photon intensity of each spectrum, it contributes to about 20% of the total $(\mu_{en}/\rho)_{air}$ for each spectrum. Because of the potential

errors associated with evaluating the $(\mu_{en}/\rho)_{air}$ for the x-ray spectra, particularly with estimating the contributions from the lower energy portions of the spectra, these values were not used in the calculations. Using higher values for $(\mu_{en}/\rho)_{air}$ would have resulted in relative response calculations that are correspondingly lower, since this variable is located in the denominator of Eq. (8). Although using a higher $(\mu_{en}/\rho)_{air}$ for the M150 spectrum may have resulted in EGS4 calculations that were in closer agreement with the experimental data, it could only have increased the discrepancy for the case of the H150 x-ray spectrum.

The fifth cause considered is unrelated to the EGS4 code and has to do only with the $CaSO_4$:Dy TL material. The photon energy dependence of $CaSO_4$:Dy is given by Eq. (1), Section 2.2. The term $\eta(E)$ in this equation is the energy-dependent relative TL efficiency. Although values for $\eta(E)$ for $CaSO_4$:Dy have been reported, the data are incomplete and inconsistent. For example values for η(100 keV) have been reported to be 0.84 [(Aypar 1978) and (Furetta and Gennai 1981)], 1.14 (McDougall and Axt 1973), and 1.22 (Pradhan et al. 1978). Due to a lack of consistent data for $\eta(E)$ for $CaSO_4$:Dy, $\eta(E)$ was assumed to be unity, which infers that the TL response is solely a function of energy deposited in the phosphor, with no other contributing factors. This assumption is also used in Eq. (8) in the calculation of the TLD response. This assumption, if invalid, could be the primary cause of the discrepancies between the EGS4 calculations and the experimental data. Variables such as phosphor grain size and LET may affect the value of $\eta(E)$.

4. SUMMARY AND CONCLUSIONS

4.1 Summary

The energy dependence of three TLDs was studied. Each TLD consisted of duplicate capsules containing powder $CaSO_4$:Dy TL material in conjunction with one of three metal energy compensation filters, 0.076 cm cadmium, 0.159 cm brass, or 0.260 cm brass. The relative responses of each dosimeter to two different x-ray spectra, beam codes M150 and H150, were determined experimentally.

A comparison of these values with those calculated using an analytical technique revealed significant differences. The calculated values were low compared with the measured values in all cases. It was initially thought that the cause for the discrepancies may be due solely to limitations in the analytical method. The analytical method required several simplifying assumptions, which have been discussed.

The EGS4 Monte Carlo code was therefore selected to improve the calculations. A user code was written that modeled each dosimeter type and x-ray code. The relative responses of the modeled dosimeters were calculated using output from EGS4 simulations. The EGS4-calculated values were in closer agreement with the measured values than the analytically-calculated values; however, discrepancies still existed. Several potential causes were identified, only one of which might adequately explain the discrepancies. The conclusion discussed below is that the energy-dependent relative TL efficiency, $\eta(E)$, is significantly different than unity for $CaSO_4$:Dy.

4.2 Conclusions

Since the available data for $\eta(E)$ is scarce and inconsistent for $CaSO_4$:Dy, it was assumed to be unity in all of the calculations. This basic assumption is believed to be invalid. Due to the apparent importance of $\eta(E)$, the original objective as discussed in Section 1.4 was not realized. That is, a single filter TLD using $CaSO_4$:Dy that would satisfy the ANSI N545-1975 energy dependence criteria was not developed using Monte Carlo methods. Instead, it is likely that $\eta(E)$ is significantly different than unity for the x-ray spectra studied.

In theory, $\eta(E)$ should be equal to the measured response divided by the calculated response.

$$\eta(E) = \frac{\text{measured response}}{\text{calculated response}} \tag{9}$$

Table 6 lists $\eta(E)$ values for the two x-ray spectra for each dosimeter studied. These values were calculated by applying data from Table 5 to Eq. (9).

Table 6. Estimated energy-dependent relative TL efficiency, $\eta(E)$, for metal-filtered $CaSO_4$:Dy TLDs to M150 and H150 x-rays.

Filter description		$\eta(E)$	$\eta(E)$
Material	Thickness	M150 x-rays	H150 x-rays
Cadmium	0.076 cm	0.81	1.26
Brass	0.159 cm	0.95	1.15
Brass	0.260 cm	0.84	1.25

Since the experimental dosimeters used in this study were filtered by either brass or cadmium, which altered the quality of the original x-ray beam, it is not possible to reach any strong conclusions as to the actual values of $\eta(E)$ for these x-ray beams. The data does suggest, however, that $\eta(E)$ is significantly larger than unity for the H150 x-ray spectrum. Recalling the discussion relating to potential errors associated with the accuracy of $(\mu_{en}/\rho)_{air}$ for the x-ray spectra, it is more difficult to reach similar conclusions regarding the M150 spectrum. Let it suffice to say that the values for $\eta(E)$ in Table 6 should be considered to be minimum values.

The accuracy of Monte Carlo methods for TLD response calculations is very dependent on an accurate knowledge of $\eta(E)$ for the TL materials of interest. Any response calculation, whether it be Monte Carlo or analytical, can only be as accurate as the knowledge of $\eta(E)$.

4.3 Suggested further studies

The most obvious suggestion would be to experimentally determine the energy-dependent relative TL efficiency, $\eta(E)$, for specific TL materials. This could be accomplished by exposing unfiltered TLDs to known doses from mono-energetic photon sources. $\eta(E)$ values for x-ray spectra could also be determined using the same method. The $\eta(E)$ values for LiF have been more intensely studied and are more thoroughly documented (Tochilin et al. 1968; Endres 1970; Rossiter 1975; Puite 1976; Budd et al. 1979; Liu 1980; Pradhan 1989; Olko 1993; Bilski 1994). If $\eta(E)$ were accurately known for $CaSO_4$:Dy, Monte Carlo codes could be used to not only keep track of total energy deposited, but also the energy of the photons depositing the energy or the linear energy

transfer (LET) distribution. In this way, corrections for $\eta(E)$ could be made, allowing for precise calculations of TLD response.

Another approach to this problem may be to use Monte Carlo methods to simulate the thermoluminescent process itself (Kulkarni 1994). By modeling the electron trapping mechanism within the crystal lattice of the TLD, it may be possible to calculate $\eta(E)$ for specific phosphors.

REFERENCES

American National Standard. Performance, testing, and procedural specifications for thermoluminescence dosimetry. ANSI N545; 1975.

American National Standard. American national standard for dosimetry - personnel dosimetry performance - criteria for testing. ANSI 1311; 1993.

Attix, F. G. Introduction to radiological physics and radiation dosimetry. New York; John Wiley and Sons; 1986.

Aypar, A. Studies on thermoluminescent $CaSO_4$:Dy for dosimetry, Int. J. Appl. Radiat. Isot., 29, 369; 1978.

Bacci, C. and Bernabei, R. Calculated energy response of some RTL detectors with multi-element filters. Radiat. Prot. Dosim., 1, 2:129, 1981.

Bassi, P., Busuoli, G., and Rimondi, O. Calculated energy dependence of some RTL and RPL detectors. Int. J. Appl. Radiat. Isot., 27:291; 1976.

Bielajew, A. F. and Rogers, D. W. O. Photoelectron angular distribution in the EGS4 code system. National Research Council of Canada, PIRS-0058; 1986.

Bilski, P., Olko, P., Burgkhardt, B., Piesch, E., and Waligorski, M. P. R. Thermoluminescence efficiency of LiF:Mg,Cu,P (MCP-N) detectors to photons, beta electrons, alpha particles and thermal neutrons. Radiat. Prot. Dosim., 55, 1:31; 1994.

Budd, T., Marshall, M., People, L. H. J., and Douglas, J. A. The low and high temperature response of LiF dosimeters to X-rays. Phys. Med. Biol., 24, 71; 1979.

Endres, G. W. R., Kathren, R. L., and Kocher, L. F. Thermoluminescence personnel dosimetry at Hanford. II. Energy dependence and application of TLD materials in operational health physics. Health Phys., 18, 665; 1970.

Furetta, C. and Gennai, P. An extensive study on the dosimetric properties of $CaSO_4$:Dy, TLD-900, in low dose region, Health Phys., 41, 674; 1981.

Horowitz, Yigal S. Thermoluminescence and thermoluminescent dosimetry, Vols. 1-3. CRC Press; 1984.

Israel, H. I. and Storm, E. Photon cross sections from 1 keV to 100 MeV for elements Z=1 to Z=100. Nuclear Data Tables A7, 565; 1970.

Klein, O. and Nishina, Y. Über die streuung von strahlung durch freie electronen nach der neuen relativistischen quantum dynamic von dirac, Z. für Physik 25, 853; 1929.

Kulkarni, R. N. The development of the Monte Carlo method for the calculation of the thermoluminescence intensity and the thermally stimulated conductivity. Radiat. Prot. Dosim., 51, 2:95; 1994.

Koch, H. W. and Motz, J. W. Bremsstrahlung cross-section formulas and related data. Rev. Mod. Phy., 31, 920; 1959.

Liu, N. H., Gilliam, J. D., and Anderson, D. W. Response of LiF thermoluminescent dosimeters to ^{99m}Tc gamma rays, Health Phys., 38, 359; 1980.

McDougall, R. S. and Axt, J. C. A preliminary evaluation fo $CaSO_4$:Dy thermoluminescent dosimeters, Health Phys., 25, 162; 1973.

Molière, G. Z. Theorie der streuung schneller geladener teilchen II. mehrfach- und vielfachstreuung. Z. Naturforsch, 3a, 78; 1948.

Motz, J. W., Olsen, H. A., and Koch, H. W. Pair production by photons, Rev. Mod. Phy., 41, 581; 1969.

Nelson, W. R., Hirayama, H., and Rogers, D. W. O. The EGS4 code system. Staford Linear Accelerator Center; SLAC-265; 1985.

Olko, P., Bilski, P., Ryba, E., and Niewiadomski, T. Microdosimetric interpretation of the anomalous photon energy response of ultra-sensitive LiF:Mg,Cu,P TL dosemeters. Radiat. Prot. Dosim., 47, 1-4:31; 1993.

Pradhan, A. S. and Bhatt, R. C. Metal filters for the compensation of photon energy dependence of the response of $CaSO_4$:Dy - teflon TLD discs. Nucl. Instrum. and Methods, 166, 497; 1979.

Pradhan, A. S. and Bhatt, R. C. Thermoluminescence response of LiF:Mg,Cu,P and LiF TLD-100 to thermal neutrons, ^{241}Am alphas and gamma rays. Radiat. Prot. Dosim., 27, 3:185; 1989.

Pradhan, A. S., Kher, R. K., Dere, A., and Bhatt, R. C. Photon energy dependence of $CaSO_4$:Dy embedded teflon TLD discs, Int. J. Appl. Radiat. Isot., 29, 243, 1978.

Puite, K. J. A thermoluminescence system for the intercomparison of absorbed dose and radiation quality of x-rays with a HVL of 0.1 to 3.0 mm Cu. Phys. Med. Biol., 21, 216; 1976.

Rossiter, M. J. The use of precision thermoluminescence dosimetry for intercomparison of absorbed dose. Phys. Med. Biol., 20, 735; 1975.

Tochilin, E., Goldstein, N., and Lyman, J. T. The quality and LET dependence of three thermoluminescent dosimeters and their potential use as secondary standards, in Proc. 2nd Int. Conf. Luminescence Dosimetry, U.S. A.E.C. CONF-680920, NTIS, Springfield, Va., 424; 1968.

Webb, G. A. M., Douch, J. C., and Bodin, G. Operational evaluation of a new high sensitivity thermoluminescent dosimeter. Health Phys., 23, 89; 1972.

Appendix A

Energy dependence of bare $CaSO_4$:Dy

MeV	Ca μ_{en}/ρ	S μ_{en}/ρ	O μ_{en}/ρ	Dy μ_{en}/ρ	μ_{en}/ρ $CaSO_4$:Dy	μ_{en}/ρ air	Relative response
0.01	86.6	48.1	5.35	258	39.78353	4.61	8.63
0.02	12	6.13	0.597	43.4	5.33541	0.511	10.44
0.03	3.57	1.78	0.168	14.4	1.575646	0.148	10.65
0.04	1.51	0.737	0.0729	6.64	0.664735	0.0668	9.95
0.05	0.776	0.373	0.0428	3.61	0.343179	0.0406	8.45
0.06	0.445	0.219	0.0313	4.98	0.207274	0.0305	6.80
0.08	0.191	0.099	0.0242	3.16	0.097335	0.0243	4.01
0.10	0.106	0.0595	0.0232	2.01	0.060208	0.0234	2.57
0.15	0.0478	0.0344	0.0248	0.796	0.03542	0.025	1.42
0.20	0.0361	0.0305	0.0266	0.395	0.031069	0.0268	1.16
0.30	0.0314	0.0296	0.0287	0.158	0.029964	0.0287	1.04
0.40	0.0306	0.0298	0.0295	0.0878	0.030004	0.0295	1.02
0.50	0.0303	0.03	0.0298	0.0613	0.030048	0.0296	1.02
0.60	0.0299	0.0297	0.0295	0.0484	0.029692	0.0295	1.01
0.80	0.0288	0.0286	0.0287	0.0359	0.02871	0.0289	0.99
1.00	0.0278	0.0279	0.0279	0.03	0.027864	0.0278	1.00
1.50	0.0254	0.0253	0.0254	0.0421	0.025401	0.0254	1.00

μ_{en}/ρ of $CaSO_4$:Dy determined by taking a weighted average of the contributions from each element. (Table 2 lists percent by weight of each element.) Relative response was calculated as the ratio of the mass energy absorption coefficients of $CaSO_4$:Dy and air. The response was normalized to 1.25 MeV.

Appendix B1

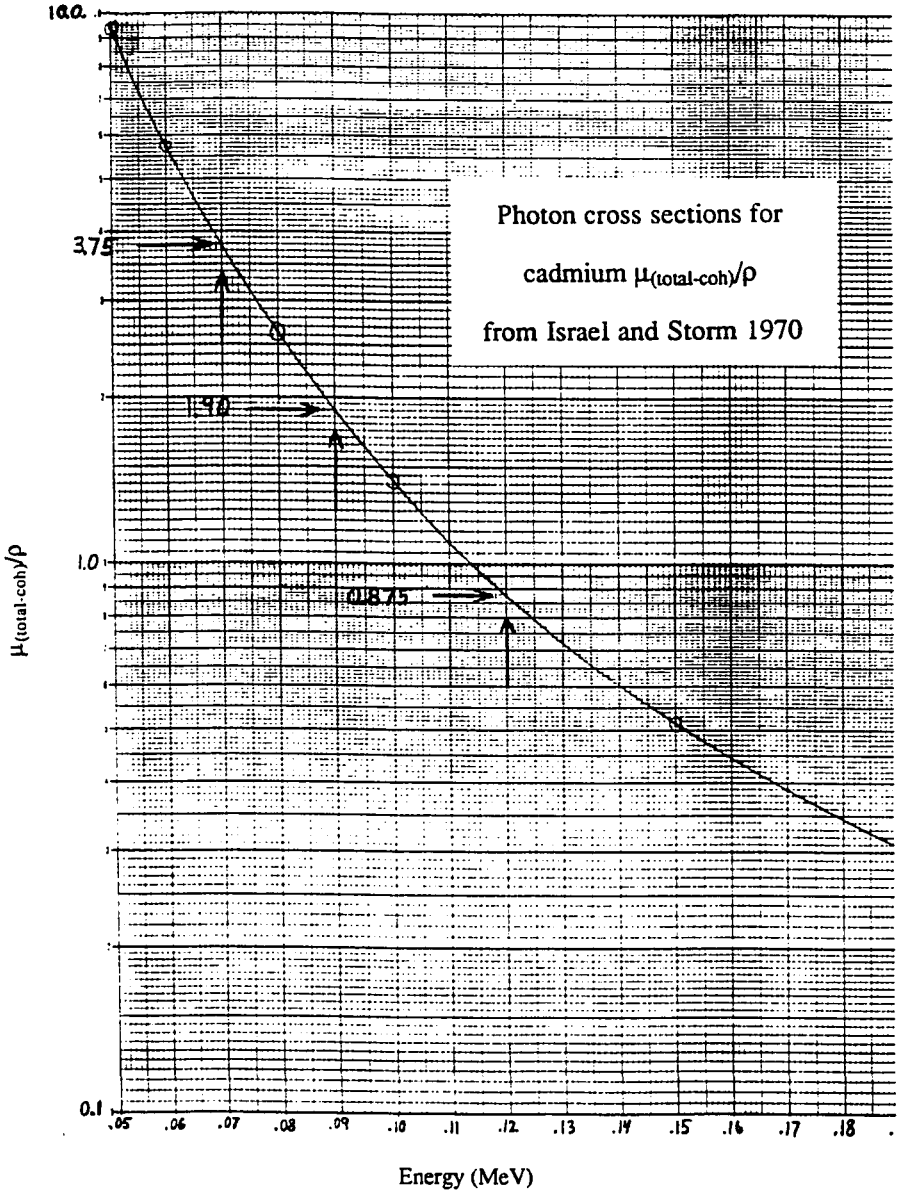

Plot indicating how the values for $\mu_{(total-coh)}/\rho$ for cadmium were determined using graphical interpolation for photon energies of 0.07, 0.09, and 0.12 MeV.

Appendix B2

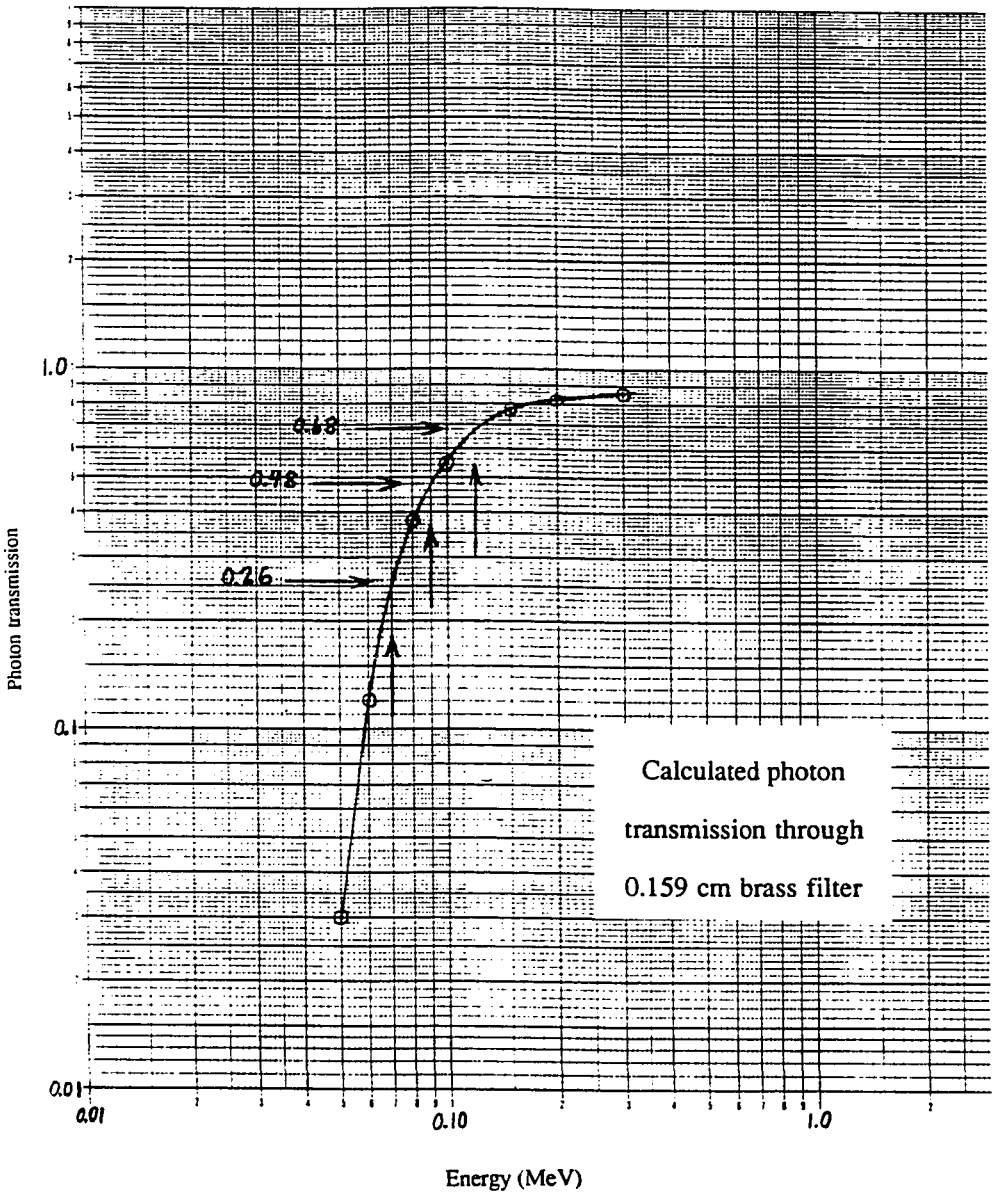

Plot indicating how the values for photon transmission through the 0.159 cm brass filter were determined using graphical interpolation for photon energies of 0.07, 0.09, and 0.12 MeV.

Appendix B3

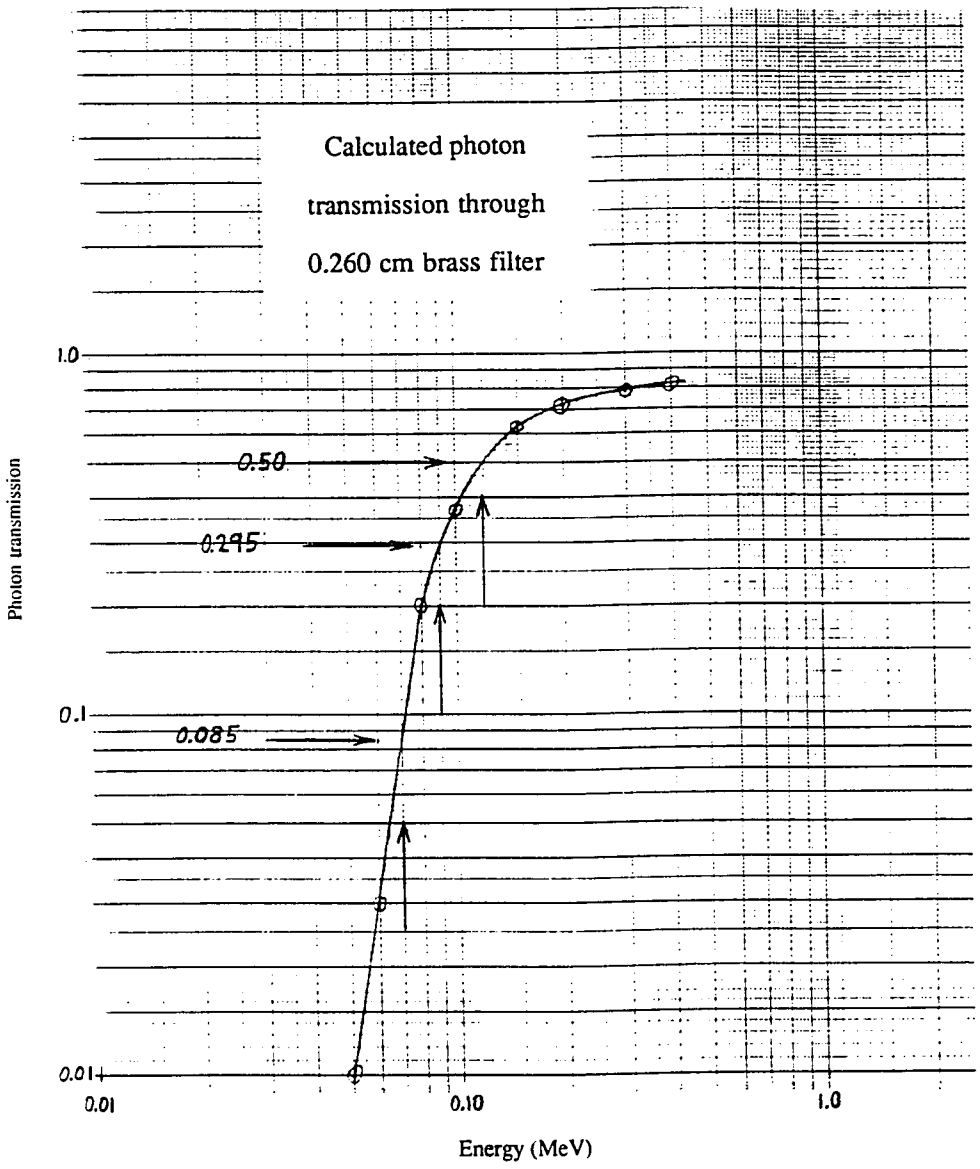

Plot indicating how the values for photon transmission through the 0.260 cm brass filter were determined using graphical interpolation for photon energies of 0.07, 0.09, and 0.12 MeV.

Appendix C1

Calculated response of $CaSO_4$:Dy behind 0.076 cm cadmium filter

Energy (MeV)	Cadmium μ/ρ (total-coh)	Transmission	Unfiltered $CaSO_4$:Dy response	Filtered dosimeter response	Response normalized to 1.25 MeV
0.05	9.44	0.0	8.45	0.02	0.02
0.06	5.74	0.0	6.80	0.15	0.16
0.07	3.75[1]	0.1	5.10	0.43	0.45
0.08	2.62	0.2	4.01	0.71	0.74
0.09	1.9[1]	0.3	3.05	0.87	0.90
0.10	1.42	0.4	2.57	1.01	1.04
0.12	0.875[1]	0.6	1.90	1.07	1.10
0.15	0.511	0.7	1.42	1.01	1.05
0.20	0.277	0.8	1.16	0.97	1.00
0.30	0.144	0.9	1.04	0.95	0.98
0.40	0.106	0.9	1.02	0.95	0.98
0.50	0.0879	0.9	1.02	0.96	1.00
0.60	0.0772	1.0	1.01	0.96	0.99
0.80	0.0647	1.0	0.99	0.95	0.98
1.00	0.0571	1.0	1.00	0.96	1.00
1.50	0.0461	1.0	1.00	0.97	1.00

[1] Interpolated values. See curve, Appendix B1.

Dosimeter response determined by multiplying the photon transmission through the filter at each energy by the corresponding unfiltered response of $CaSO_4$:Dy (See the last column of Appendix A). The response was then normalized to 1.25 MeV.

Appendix C2

Calculated response of $CaSO_4$:Dy behind 0.159 cm brass filter

Energy (MeV)	330 brass components: copper 66.5% μ/ρ (ttl-coh)	zinc 33.0% μ/ρ (ttl-coh)	lead 0.5% μ/ρ (ttl-coh)	Weighted average 330 brass μ/ρ (ttl-coh)	Transmission	Unfiltered $CaSO_4$:Dy response	Filtered dosimeter response	Response normalized to 1.25 MeV
0.05	2.44	2.71	7.25	2.55	0.03	8.45	0.27	0.29
0.06	1.48	1.63	4.46	1.54	0.12	6.80	0.84	0.91
0.07					0.26[1]	5.10	1.33	1.42
0.08	0.691	0.766	2.08	0.723	0.38	4.01	1.51	1.62
0.09					0.48[1]	3.05	1.46	1.57
0.10	0.41	0.448	5.33	0.447	0.55	2.57	1.40	1.51
0.12					0.68[1]	1.90	1.29	1.39
0.15	0.2	0.21	1.92	0.21	0.75	1.42	1.07	1.15
0.20	0.143	0.149	0.94	0.149	0.82	1.16	0.95	1.02
0.30	0.106	0.109	0.375	0.108	0.86	1.04	0.90	0.97
0.40	0.0909	0.0919	0.215	0.0919	0.88	1.02	0.90	0.97
0.50	0.0815	0.0823	0.15	0.0821	0.89	1.02	0.91	0.98
0.60	0.0748	0.0754	0.117	0.0752	0.90	1.01	0.91	0.98
0.80	0.0652	0.0657	0.0842	0.0655	0.92	0.99	0.91	0.97
1.00	0.0584	0.0588	0.0681	0.0586	0.92	1.00	0.92	0.99
1.50	0.0477	0.048	0.0506	0.0478	0.94	1.00	0.94	1.01

density (ρ) of brass = 8.5 g/cm^3

[1]Interpolated values. See curve, Appendix B2.

Dosimeter response determined by multiplying the photon transmission through the filter at each energy by the corresponding unfiltered response of $CaSO_4$:Dy (See the last column of Appendix A). The response was then normalized to 1.25 MeV. μ_{en}/ρ of brass is determined by taking a weighted average of the contributions from each element.

Appendix C3

Calculated response of $CaSO_4$:Dy behind 0.260 cm brass filter

Energy (MeV)	330 brass components: copper 66.5% μ/ρ (ttl-coh)	zinc 33.0% μ/ρ (ttl-coh)	lead 0.5% μ/ρ (ttl-coh)	Weighted average 330 brass μ/ρ (ttl-coh)	Transmission	Unfiltered $CaSO_4$:Dy response	Filtered dosimeter response	Response normalized to 1.25 MeV
0.05	2.44	2.71	7.25	2.55	0.00	8.45	0.03	0.03
0.06	1.48	1.63	4.46	1.54	0.03	6.80	0.22	0.25
0.07					0.09[1]	5.10	0.43	0.49
0.08	0.691	0.766	2.08	0.723	0.20	4.01	0.81	0.91
0.09					0.30[1]	3.05	0.90	1.01
0.10	0.41	0.448	5.33	0.447	0.37	2.57	0.96	1.08
0.12					0.50[1]	1.90	0.95	1.07
0.15	0.2	0.21	1.92	0.21	0.63	1.42	0.89	1.00
0.20	0.143	0.149	0.94	0.149	0.72	1.16	0.83	0.94
0.30	0.106	0.109	0.375	0.108	0.79	1.04	0.82	0.92
0.40	0.0909	0.0919	0.215	0.0919	0.82	1.02	0.83	0.94
0.50	0.0815	0.0823	0.15	0.0821	0.83	1.02	0.85	0.96
0.60	0.0748	0.0754	0.117	0.0752	0.85	1.01	0.86	0.96
0.80	0.0652	0.0657	0.0842	0.0655	0.87	0.99	0.86	0.96
1.00	0.0584	0.0588	0.0681	0.0586	0.88	1.00	0.88	0.99
1.50	0.0477	0.048	0.0506	0.0478	0.90	1.00	0.90	1.01

density (ρ) of brass = 8.5 g/cm^3

[1]Interpolated values. See curve, Appendix B3.

Dosimeter response determined by multiplying the photon transmission through the filter at each energy by the corresponding unfiltered response of $CaSO_4$:Dy (See the last column of Appendix A). The response was then normalized to 1.25 MeV. μ_{en}/ρ of brass is determined by taking a weighted average of the contributions from each element.

Appendix D

Energy dependence of bare $CaSO_4$:Dy (just capsules) using EGS4

Energy (Mev)	Fractional energy deposited		Average	μ_{en}/ρ	Relative
	Region 5	Region 7	Regions 5 & 7	(air)	response
0.01	0.0505000	0.0502000	0.05035	4.61	0.44
0.02	0.0516700	0.05181	0.05174	0.511	4.11
0.03	0.0310600	0.03093	0.030995	0.148	8.50
0.05	0.0092920	0.009163	0.0092275	0.0406	9.23
0.08	0.0027060	0.002685	0.0026955	0.0243	4.50
0.10	0.0016650	0.001645	0.001655	0.0234	2.87
0.15	0.0010000	0.001003	0.0010015	0.025	1.63
0.20	0.0008867	0.0008901	0.0008884	0.0268	1.35
0.50	0.0008694	0.0008738	0.0008716	0.0296	1.20
1.00	0.0007453	0.0007617	0.0007535	0.0278	1.10
1.25	0.0006476	0.0006630	0.0006553	0.0266	1.00

Relative response is calculated using Eq. (8), where f(E) is the average fractional energy deposited in regions 5 & 7.

Appendix E1

EGS4 calculation of energy dependence of $CaSO_4$:Dy with 0.076 cm cadmium filter (with K edge x-ray and PE angular sampling)

Energy (Mev)	Fractional energy deposited Region 5	Region 7	Average Regions 5 & 7	μ_{en}/ρ (air)	Relative response
0.07	0.0006336	0.0006311	0.0006324	0.0274	0.57
0.08	0.0009915	0.0008724	0.0009320	0.0243	0.94
0.09	0.001244	0.001267	0.0012555	0.0239	1.29
0.10	0.0012340	0.001314	0.0012740	0.0234	1.34
0.12	0.0013740	0.001391	0.0013825	0.0240	1.42
0.13	0.0012960	0.001373	0.0013345	0.0244	1.35
0.15	0.0012560	0.001288	0.0012720	0.0250	1.25
0.20	0.0011850	0.001169	0.0011770	0.0268	1.08
0.66	0.0012460	0.001215	0.0012305	0.0293	1.03
1.25	0.0010410	0.00112	0.0010805	0.0266	1.00
M150	0.0009636	0.001042	0.0010028	0.0274	0.90
H150	0.0012950	0.001211	0.0012530	0.0240	1.29

Relative response is calculated using Eq. (8), where f(E) is the average fractional energy deposited in regions 5 & 7.

Appendix E2

EGS4 calculation of energy dependence of $CaSO_4$:Dy with 0.159 cm brass filter (with K edge x-ray and PE angular sampling)

Energy (Mev)	Fractional energy deposited Region 5	Region 7	Average Regions 5 & 7	μ_{en}/ρ (air)	Relative response
0.06	0.0008234	0.0007929	0.0008082	0.0305	0.84
0.07	0.0011460	0.0011580	0.0011520	0.0274	1.33
0.08	0.0011710	0.0011350	0.0011530	0.0243	1.50
0.09	0.0011910	0.0011360	0.0011635	0.0239	1.54
0.10	0.0012130	0.0011710	0.0011920	0.0234	1.61
0.12	0.0010620	0.0011120	0.0010870	0.0240	1.43
0.13	0.0010450	0.0010700	0.0010575	0.0244	1.37
0.15	0.0010020	0.0009949	0.0009985	0.0250	1.26
0.20	0.0009204	0.0009174	0.0009189	0.0268	1.08
0.66	0.0009065	0.0009393	0.0009229	0.0293	0.99
1.25	0.0008423	0.0008428	0.0008426	0.0266	1.00
M150	0.0011220	0.001033	0.0010775	0.0274	1.24
H150	0.0010760	0.001092	0.0010840	0.0240	1.43

Relative response is calculated using Eq. (8), where f(E) is the average fractional energy deposited in regions 5 & 7.

Appendix E3

EGS4 calculation of energy dependence of $CaSO_4$:Dy with 0.260 cm brass filter (with K edge x-ray and PE angular sampling)

Energy (Mev)	Fractional energy deposited Region 5	Region 7	Average Regions 5 & 7	μ_{en}/ρ (air)	Relative response
0.06	0.0001455	0.0001424	0.0001440	0.0305	0.20
0.07	0.0003022	0.0003877	0.0003450	0.0274	0.52
0.08	0.0005322	0.0005210	0.0005266	0.0243	0.90
0.09	0.0005853	0.0006024	0.0005939	0.0239	1.03
0.10	0.0006716	0.0005801	0.0006259	0.0234	1.11
0.12	0.0007064	0.0007020	0.0007042	0.0240	1.22
0.13	0.0007151	0.0006700	0.0006926	0.0244	1.18
0.15	0.0006906	0.0006847	0.0006877	0.0250	1.14
0.20	0.0006969	0.0007139	0.0007054	0.0268	1.09
0.66	0.0006900	0.0006817	0.0006859	0.0293	0.97
1.25	0.0006407	0.0006407	0.0006407	0.0266	1.00
M150	0.0005454	0.000512	0.0005287	0.0274	0.80
H150	0.0006548	0.0006181	0.0006365	0.0240	1.10

Relative response is calculated using Eq. (8), where f(E) is the average fractional energy deposited in regions 5 & 7.

Appendix F1

EGS4 calculation of energy dependence of $CaSO_4$ with 0.076 cm cadmium filter (without K edge or PE angular sampling)

Energy (Mev)	Fractional energy deposited Region 5	Region 7	Average Regions 5 & 7	μ_{en}/ρ (air)	Relative response
0.06	0.0001143	0.0001473	0.0001308	0.0305	0.14
0.07	0.0002941	0.0003238	0.0003090	0.0274	0.37
0.08	0.0004623	0.0005378	0.0005001	0.0243	0.68
0.10	0.0007531	0.0006365	0.0006948	0.0234	0.98
0.12	0.0007659	0.0007382	0.0007521	0.0240	1.03
0.15	0.0008015	0.0008248	0.0008132	0.0250	1.07
0.66	0.0008718	0.0009098	0.0008908	0.0293	1.00
1.25	0.0008061	0.0008061	0.0008061	0.0266	1.00

Relative response is calculated using Eq. (8), where f(E) is the average fractional energy deposited in regions 5 & 7.

Appendix F2

EGS4 calculation of energy dependence of $CaSO_4$ with 0.159 cm brass filter (without K edge or PE angular sampling)

Energy (Mev)	Fractional energy deposited Region 5	Region 7	Average Regions 5 & 7	μ_{en}/ρ (air)	Relative response
0.05	0.0002175	0.0002633	0.0002404	0.0406	0.24
0.07	0.0007770	0.0008875	0.0008323	0.0274	1.21
0.08	0.0009280	0.0009589	0.0009435	0.0243	1.54
0.10	0.0008947	0.0009037	0.0008992	0.0234	1.53
0.12	0.0008905	0.0008299	0.0008602	0.0240	1.43
0.15	0.0007669	0.0007810	0.0007740	0.0250	1.23
0.20	0.0007429	0.0007364	0.0007397	0.0268	1.10
0.66	0.0007058	0.0007298	0.0007178	0.0293	0.97
1.25	0.0006671	0.0006706	0.0006689	0.0266	1.00

Relative response is calculated using Eq. (8), where f(E) is the average fractional energy deposited in regions 5 & 7.

Appendix F3

EGS4 calculation of energy dependence of $CaSO_4$ with 0.260 cm brass filter (without K edge or PE angular sampling)

Energy (Mev)	Fractional energy deposited Region 5	Region 7	Average Regions 5 & 7	μ_{en}/ρ (air)	Relative response
0.04	0.0000012	0.0000000	0.0006	0.0668	0.00
0.06	0.0001393	0.0001078	0.1236	0.0305	0.20
0.07	0.0003354	0.0003001	0.3178	0.0274	0.58
0.08	0.0004165	0.0004367	0.4266	0.0243	0.88
0.09	0.0004348	0.0004965	0.4657	0.0239	0.97
0.10	0.0005347	0.0005543	0.5445	0.0234	1.16
0.11	0.0005036	0.0005673	0.5355	0.0237	1.13
0.12	0.0005402	0.0005654	0.5528	0.024	1.15
0.13	0.0005595	0.0005455	0.5525	0.0244	1.13
0.14	0.0005873	0.0005551	0.5712	0.0247	1.16
0.15	0.0005828	0.0005770	0.5799	0.025	1.16
0.20	0.0005719	0.0005768	0.5744	0.0268	1.07
0.30	0.0005765	0.0005754	0.576	0.0287	1.00
0.50	0.0006252	0.0005657	0.5955	0.0296	1.01
0.66	0.0005900	0.0005608	0.5754	0.0293	0.98
1.00	0.0005180	0.0005369	0.5275	0.0278	0.95
1.25	0.0005373	0.0005265	0.5319	0.0266	1.00

Relative response is calculated using Eq. (8), where f(E) is the average fractional energy deposited in regions 5 & 7.

Appendix G1

EGS4 calculation of energy dependence of $CaSO_4$:Dy with 0.159 cm brass filter (with K edge x-ray and without PE angular sampling)

Energy (Mev)	Fractional energy deposited Region 5	Region 7	Average Regions 5 & 7	μ_{en}/ρ (air)	Relative response
0.06	0.0007825	0.0007549	0.0007687	0.0305	0.81
0.07	0.0010570	0.0011450	0.0011010	0.0274	1.30
0.08	0.0012830	0.0012860	0.0012845	0.0243	1.71
0.10	0.0012260	0.0011600	0.0011930	0.0234	1.65
0.12	0.0009846	0.0010740	0.0010293	0.0240	1.39
0.15	0.0010140	0.0009712	0.0009926	0.0250	1.28
0.20	0.0009408	0.0009510	0.0009459	0.0268	1.14
0.66	0.0009500	0.0009625	0.0009563	0.0293	1.05
1.25	0.0008209	0.0008259	0.0008234	0.0266	1.00

Relative response is calculated using Eq. (8), where f(E) is the average fractional energy deposited in regions 5 & 7.

Appendix G2

EGS4 calculation of energy dependence of $CaSO_4$:Dy with 0.260 cm brass filter (with K edge x-ray and without PE angular sampling)

Energy (Mev)	Fractional energy deposited Region 5	Region 7	Average Regions 5 & 7	μ_{en}/ρ (air)	Relative response
0.06	0.0001374	0.0001612	0.0001493	0.0305	0.21
0.07	0.0003901	0.0003503	0.0003702	0.0274	0.57
0.08	0.0005392	0.0005486	0.0005439	0.0243	0.94
0.09	0.0006191	0.0006351	0.0006271	0.0239	1.10
0.10	0.0006386	0.0006918	0.0006652	0.0234	1.19
0.12	0.0006565	0.0006454	0.0006510	0.024	1.14
0.13	0.0006906	0.0007182	0.0007044	0.0244	1.21
0.15	0.0007005	0.0006890	0.0006948	0.025	1.17
0.20	0.0006943	0.0006704	0.0006824	0.0268	1.07
0.66	0.0007252	0.0007111	0.0007182	0.0293	1.03
1.25	0.0006170	0.0006486	0.0006328	0.0266	1.00

Relative response is calculated using Eq. (8), where f(E) is the average fractional energy deposited in regions 5 & 7.